NASA TECHNICAL NOTE

NASA TN D-4805

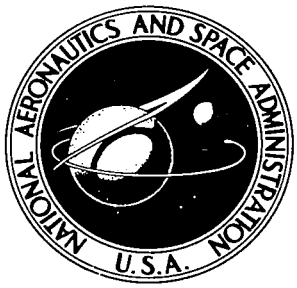

NASA TN D-4805

PRELIMINARY STUDY OF A THERMIONIC REACTOR CORE COMPOSED OF SHORT-LENGTH EXTERNALLY FUELED DIODES

by Howard G. Yacobucci

Lewis Research Center
Cleveland, Ohio

NATIONAL AERONAUTICS AND SPACE ADMINISTRATION • WASHINGTON, D. C. • SEPTEMBER 1968

PRELIMINARY STUDY OF A THERMIONIC REACTOR CORE COMPOSED OF SHORT-LENGTH EXTERNALLY FUELED DIODES

By Howard G. Yacobucci

Lewis Research Center
Cleveland, Ohio

NATIONAL AERONAUTICS AND SPACE ADMINISTRATION

For sale by the Clearinghouse for Federal Scientific and Technical Information
Springfield, Virginia 22151 – CFSTI price $3.00

ABSTRACT

The characteristics of a thermionic reactor-core concept, aimed at incorporation of the best features of several previously proposed concepts, are studied. Optimization of diode dimensions resulted in a reference design for a 200-kW electric core. The design, which employs electrical zoning to reduce the detrimental effect of radial thermal power variation, was analyzed for various electrical failures. Equations were derived for calculating internal resistance losses in diodes that have an electrical conductor in parallel with an electrode.

CONTENTS

PRELIMINARY STUDY OF A THERMIONIC REACTOR CORE COMPOSED OF SHORT-LENGTH EXTERNALLY FUELED DIODES

by Howard G. Yacobucci

Lewis Research Center

SUMMARY

Some of the problems encountered in the design of in-pile thermionic reactor cores are studied by means of a conceptual design. The design, which is preliminary in nature, utilizes fuel elements containing series-connected, short-length, externally fueled diodes. The basic requirements for the reference design are that it produce 200 kilowatts of electric power, be lithium cooled, and have shaped 4π shielding.

The detrimental effect of core thermal power variation on the performance of series strings of fuel elements was reduced by grouping the fuel elements in radial zones of nearly uniform thermal input power and operating each zone at an optimum diode current density.

Diode dimensions were optimized on a power-per-unit-cell-volume basis because of the shielding requirement. It was determined that the optimum emitter length is about 2.0 centimeters (for emitter diameters ranging from 0.5 to 2.5 centimeters) and that the emitter diameter should be kept as small as possible.

An equation was derived to determine the combined ohmic loss when an electrode of a diode and an electrical conductor are in parallel. The assumptions are that the current through the electrode varies with diode length while the current through the parallel conductor is constant.

Electrical failure analyses indicate that a limited number of short-circuited diodes results in negligible penalties. Open-circuited diodes are a more serious problem and require either reduced normal operating temperatures and larger reactor sizes or reduced postfailure power levels. Heat-transfer analyses indicate that a reference-design diode will not experience a fuel meltdown in the event of an open circuit if the emitter diameter is less than 1.30 centimeters.

An area which requires more extensive analyses and high-temperature materials development is the sealing of the cesium space from the fission-gas vent space.

INTRODUCTION

A thermionic diode is a static device that converts heat energy directly into electrical energy. Basically, a thermionic diode consists of a heated emitter which is separated from a cooled collector by a gap. Some electrons are driven from the hot emitter surface with sufficient kinetic energy to reach the collector. From there they flow back to the emitter through an external circuit while doing work in the circuit. The electron density in the interelectrode gap can build up to the point where the resulting negative space charge repels any additional electrons that try to escape from the emitter surface. If the negative space charge is not neutralized, the flow of current will be limited. Neutralization can be accomplished with the positive ions of an easily ionized alkali metal. The most common metal used for this purpose is cesium, which is introduced into the interelectrode gap as a vapor.

Several design concepts have been proposed whereby thermionic diodes are intergrated into a nuclear reactor for the purpose of producing electric power in space. All these concepts use cylindrical diodes which are either internally or externally fueled. In the former, the centrally positioned fuel is surrounded by an emitter, a collector, and the rest of the diode structure. The externally fueled diode is just the opposite; the fuel surrounds an emitter and a centrally cooled collector.

The three design concepts for in-pile thermionic space reactors that are generally considered to be the most promising are popularly referred to as (1) the "flashlight," (2) the "unit-cell pancake," and (3) the "core-length externally fueled" concepts. A brief description of each is given in the following paragraphs. A more thorough description of the design concepts and a discussion of their advantages and disadvantages are presented in reference 1.

The flashlight design uses short-length internally fueled diodes that are stacked one upon the other and series connected to form a fuel element. Many such fuel elements, cooled by liquid metal flowing axially over the outer surfaces, make up the reactor core.

In the unit-cell pancake approach, a number of internally fueled diodes are individually supported from a planar structure. Many slabs, or pancakes, of diodes are assembled to form the reactor core. With this type of design the slabs can be oriented in any direction, thus permitting either axial or radial coolant flow through the reactor core. Furthermore, the cells of a slab can be interconnected electrically in a series-parallel network. This arrangement reduces the power loss due to an open-circuited diode (in a series string of diodes) by providing alternate paths for the current.

The third concept uses core-length externally fueled diodes that must be centrally cooled due to the fuel location. Internal ohmic losses, which increase greatly with diode length, are reduced by using a double-ended diode. That is, current is taken from each end of the diode, which effectively halves the electrode length as far as ohmic losses are concerned.

The concept discussed in this report is somewhat of a hybrid of the first and third concepts while providing for the electrical interconnection advantage of the second. It might be thought of as an "externally-fueled flashlight" concept that permits series-parallel electrical connections between diodes.

In this preliminary study the advantages and limitations of this concept were investigated. A parametric study optimized the diode length and the collector thickness to provide the maximum electric power output per unit of diode cell volume. The reference design was optimized on the assumption that shaped 4π shielding will be required for manned applications.

One of the problem areas in thermionic reactor design is the detrimental effect of radial and axial thermal power variation, due to neutron leakage, on the performance of series strings of diodes. Several methods of achieving "power flattening" have been proposed (refs. 1 and 2). This report presents a method of reducing the effects of the radial power variation by employing electrical zones. The core is divided into radial zones in which the input thermal power variation is slight. The current density varies from zone to zone to extract more power from the reactor core than a uniform current density would allow.

Analyses were performed on a typical reference-design circuit to determine the effects of open-circuit and short-circuit failures on the operating conditions of the remaining diodes in the circuit. In addition, heat-transfer analyses were made on open-circuited externally and internally fueled diodes which were then compared on an equal-emitter-diameter basis.

Equations were derived to permit the calculation of internal ohmic losses when an electrical conductor is in parallel with one of the electrodes of a diode. The conventional electrical circuit analysis gives power losses that are too low. The problem is caused by variable current flow through the electrode while the current flow through the parallel conductor is constant.

Two seal designs for the reference-design fuel element were analyzed. Emphasis was placed on the stresses caused by differential axial growth on the metallic components of such seals.

DESIGN PHILOSOPHY

For a device as complex as an in-pile thermionic reactor, any conceptual design is a compromise among several important factors. The reference design discussed in this report incorporates features which, it is believed, afford solutions to the more difficult problems. The remaining problems do not appear to be insoluble. The choices made in the evolution of the reference design are discussed below along with an exploration of their advantages and disadvantages.

TABLE I. - DESIGN PARAMETERS AND

DIODE MATERIALS

Design parameters	
Temperature, K(^{o}R):	
Emitter (max.)	2000 (3600)
Collector	1400 (2520)
Diode current density (max.), A/cm^2	15
Thermal input power (max.), W/cm^2	77
Core power ratio (cosine), max./min.	
Axial	1.2
Radial	1.2
Core power output (approx.), kW electric	200
Materials	
Emitter	Tungsten
Collector	Niobium
Coolant tube	Niobium
Trilayer insulator	Alumina
Cladding	Tungsten
Coolant	Lithium

The reference-design reactor produces approximately 200 kilowatts of electric power. This reactor size is criticality limited, but until sizes are reached in which control becomes a problem, the number of fuel assemblies could be increased to produce higher-power reactors.

Table I lists the design conditions, the performance parameters, and the materials selected for this study. Performance at the design conditions was based on conservative estimates of diode power output and efficiency.

Diode Configuration

When the complexity and cost of constructing a thermionic reactor is considered, testability of the diode becomes an exceedingly important criterion. To assure reliability, the diodes should be tested after fabrication and before installation in the core. In-pile testing is impractical because of the cost and the problems involved in assembling radioactive components. These problems can be avoided by using nonnuclear heating.

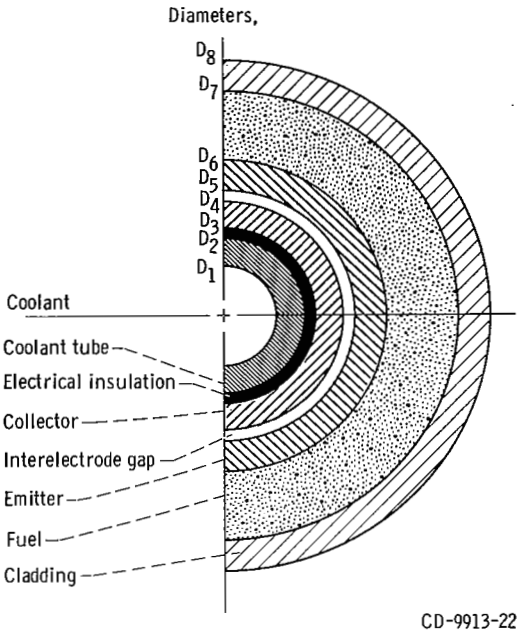

Figure 1. - Externally fueled diode cross section.

The externally fueled diode (fig. 1) readily lends itself to such heating. Since the heat path is normally from the outside in, the heat source can be easily applied. Methods are either available, or are under development, for testing internally fueled diodes; but they are more complicated or more limited than those available for externally fueled diodes. An internally fueled diode could be designed with a central cavity large enough to accept a heat source. This would make testing of the diode easier but would result in a larger reactor. Another method would be to heat the emitter before inserting the fuel, but any malfunctions resulting from the fuel insertion and final assembly process would go undetected. Completely assembled, internally fueled diodes could be tested by a back emission process which is currently being developed. Such testing will probably be more time consuming than direct heating of externally fueled diodes and will require a correlation of transient test results with desired steady-state operating conditions.

The externally fueled diode has an advantage over the internally fueled diode in the event of an open-circuit failure. Normally, a sizable portion of the fission heat generated in the fuel is converted to kinetic energy of the electrons. Loss of this "electron cooling" due to the open circuit raises the temperature of the diode because the remaining modes of heat transfer must take on additional heat loads. In thermionics, the most effective mode of heat transfer is emitter-to-collector radiation. (For a complete discussion of the various heat-transfer processes in thermionics, see ref. 2.) The difference between an internally fueled and an externally fueled diode, in the event of an open-circuit failure, lies in the radiative heat-transfer areas and the heat sinks. An internally

fueled diode can only radiate heat from the emitter to the collector. The externally fueled diode can radiate heat from its fuel cladding to its neighbor diodes, as well as from its emitter to its collector. It is shown in the section Open-Circuit Temperature Rise that this additional heat-transfer path can prevent a fuel meltdown in the reference diode while an internally fueled diode of equal emitter diameter will experience a fuel meltdown.

Another type of probable electrical failure is a short circuit caused by the closely spaced electrodes of a diode coming in contact with each other. This contact can occur by distortion of the emitter due to fuel swelling. The reference design may reduce the probability of this failure since fuel swelling does not tend to decrease the interelectrode gap. The reasons are discussed in detail in the section Fuel Selection.

With an internally fueled flashlight design, fission-gas venting is a problem since the diode structure completely encloses the fuel. Venting of the externally fueled diode is less difficult to accomplish because the fuel, being on the outside, is readily accessible. A number of alternate venting schemes are possible. The internally fueled unit-cell diode has about the same venting advantage as an externally fueled diode.

Analyses have shown that the power loss due to an open circuit can be minimized by using cross connections between diodes of adjacent series strings (ref. 3). This procedure prevents the loss of an entire circuit by providing alternate paths for the current. Interconnections between diodes can be made in the unit-cell pancake and externally fueled short-length concepts, but the internally fueled flashlight concept does not lend itself to this approach. Except for fuel meltdown, the core-length externally fueled concept has no advantage over the internally fueled flashlight concept in the event of an open circuit. Since interconnections between diodes can only be made at the reactor-core extremities, the loss of one diode is equivalent to losing a whole fuel element of the flashlight concept. If the failure were a short-circuited diode, the core-length concept is inferior to the internally fueled flashlight concept. The reason for this inferiority is that the power loss is again equivalent to losing a whole fuel element while the power loss for the internally fueled flashlight concept is only a fraction of the total fuel-element power.

As the diode length increases, the internal ohmic losses of the electrodes increase rapidly because the losses are proportional to the cube of the electrode length. The problem of high ohmic losses can be reduced by increasing the cross-sectional areas of the electrodes. Collector thickness optimization is discussed in the section OPTIMIZATION OF DIODE DIMENSIONS. Increasing the cross-sectional areas of the emitter and the cladding (if the diode is externally fueled) results in an increase in the diode cell volume and a reduction in the fuel volume fraction. This reduces the power output per unit cell volume and leads to a larger reactor for a given total power output.

Selection of short-length externally-fueled diodes for the reference design presents problems that some of the other concepts do not have. For instance, there is the possi-

bility of shorting between fuel elements due to thermal expansions of diodes and/or fuel-element distortions. Although a problem of this nature can be solved by proper design, it does not exist for an internally fueled diode. Perhaps the most serious disadvantage of the reference design is the high-temperature requirements placed on the electrical insulator-seals. The ceramic portions of such devices are not only in contact with components that operate at 2000 K (3600° R) or more, but they must also withstand long-term nuclear radiation. The core-length concept reduces the magnitude of the nuclear effects by placing the insulator-seals outside the reactor core. The internally fueled concepts reduce the temperature requirements on the insulator-seals by avoiding contact with the high-temperature emitters.

Gaseous Fission Product Venting

The reference design was made compatible with the venting of gaseous fission products from the space occupied by the fuel. For long-term reactor operation and a ceramic fuel, venting is necessary to keep destructive pressures from building up in the emitter structure. As the gaseous fission products are removed from the fuel space, vaporized fuel will also be removed. However, there is some evidence that venting can be accomplished without an excessive loss of fuel (unpublished data by P. Hill of General Electric Co.).

The reference design also assumes that the gaseous fission products are discharged directly to space. If this is not permitted, a method must be devised to remove the gases from the reactor core. One such method might be to pump the gases to a high-pressure shielded retention tank located outside the reactor core. Accumulation of the gases in the containment vessel is not desirable because of the resulting high pressures in that structure and the additional loads imposed on the seals which prevent contamination of the cesium spaces with fission products.

Fuel Selection

The high temperature levels encountered in in-pile thermionics require the use of ceramic fuels, such as uranium dioxide (UO_2), uranium carbide (UC), uranium nitride (UN), or cermets containing these fuels. The cermets may suffer a burnup limitation, are difficult to vent (should that prove to be necessary), and result in relatively large reactor cores. A reactor fueled with UN or UC will be smaller for a given power level than one fueled with UO_2. However, ceramic UO_2 (fully enriched in U^{235}) was selected for the reference design because more is known about its behavior than any of the other

fuels, and its use results in a reasonable reactor size.

The expansion coefficient of UO_2, being higher than that of tungsten, results in increases in both the internal and external fuel diameters of an externally fueled diode as it heats up. The fuel tends to pull away from the tungsten emitter rather than reduce the interelectrode gap as it might do if the diode were internally fueled. The gap created between the emitter and the fuel would result in excessively high fuel temperatures if it were not for "void migration" in the UO_2.

Void migration is the apparent movement of voids that has been found to occur in irradiated samples of UO_2 fuel. Artifical voids drilled in a UO_2 pellet migrated along radial lines toward the hot center of the pellet, as depicted in figure 2 (ref. 4). Void

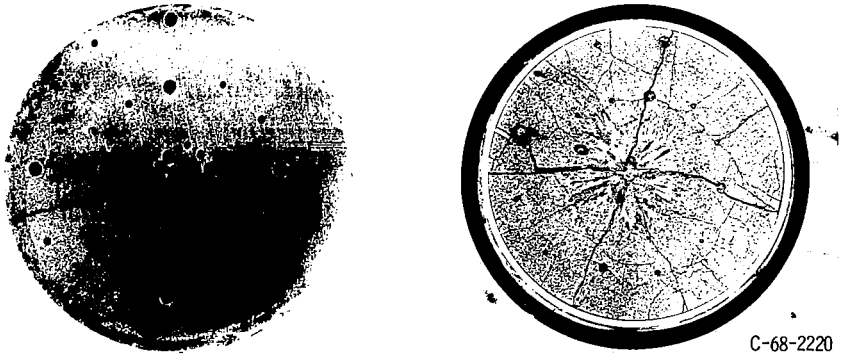

(a) Artificial voids ultrasonically drilled in UO_2 pellet before irradiation.

(b) Artificial voids after irradiation.

Figure 2. - Change in void distribution in UO_2 pellet.

migration occurs when the temperature level is high enough and a thermal gradient exists which causes a vaporizing-condensing process to take place between the relatively hot and cold surfaces of the fuel surrounding the voids. That is, UO_2 vaporizes from the hot edge of the void, diffuses across the void, and redeposits on the cold side (ref. 4).

Since the fuel of an externally fueled diode is hottest on the exterior (cladding) surface and coolest on the interior (emitter) surface, it can be expected that any gap between the emitter surface and the fuel will be filled with redeposited UO_2. The thermal bond between the redeposited UO_2 and the emitter should be good judging from the results of the pellet tests. Note in figure 2 that the parent UO_2 cracked while the bond was intact after irradiation. A good bond means little temperature rise across the emitter-fuel interface and a lower maximum fuel temperature.

The migration of voids to the hottest regions of the fuel as observed in these tests also indicates advantages in venting gaseous fission products. Any voids in the as-

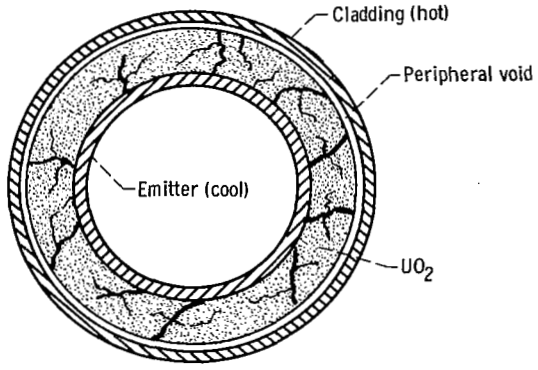

Figure 3. - Assumed post irradiation appearance of externally fueled UO_2 diode.

fabricated UO_2, or those resulting from fission product generation, will be swept to the outer periphery of the fuel, carrying fission gases with them (see fig. 3). Venting can then be accomplished through openings in the cladding.

A problem may result from this generally beneficial migration of fuel. At operating temperatures the fuel is in intimate contact with the emitter surface. When the reactor is subsequently shut down, the higher expansion coefficient of UO_2 will result in its exerting an external force on the emitter. The emitter must be made thick enough to resist buckling as the UO_2 shrinks around it. Since the emitter tends to cool faster than the UO_2, the strength requirement is based on lower than the maximum emitter temperature. Temperature gradients within the UO_2 should induce cracking of the brittle fuel, as shown in figure 3. Out-of-pile cyclic testing could be used to establish the emitter thickness required to resist buckling due to this difference in contraction at shutdown.

Cesium Supply System

While it is recognized that the self-regulated integral cesium reservoir (ref. 5) has many potential advantages over the external reservoir, more research and development is required. Therefore, the external cesium reservoir is used in the reference design. That is, cesium reservoirs with their necessary temperature controls are located outside the reactor core, and the cesium is supplied to interconnected strings of fuel elements by means of small-diameter tubing.

If, in the future, the self-regulated integral cesium reservoir proves to be satisfactory, it will be a simple matter to remove from the design the heaters, the coolant loops, and the plumbing required for the external cesium reservoirs. In that case, each diode fuel-element module would have its own built-in, self-regulated reservoir.

OPTIMIZATION OF DIODE DIMENSIONS

In any space application size and weight of the system are of utmost importance. If the vehicle is to be manned, shaped 4π shielding of the reactor may be required. In this case, the reactor-core volume must be minimized to reduce the shield weight which will be a considerable portion of the total system weight.

The size of a thermionic reactor is essentially determined by criticality requirements, temperature limitations, diode performance, and the electrical power level. The electrical power level and diode performance determine the total emitter surface area required. The volume of fuel per unit emitter surface area must be high enough to satisfy the criticality requirements and low enough to maintain reasonable fuel temperatures.

A series of parametric studies was carried out in an attempt to determine the diode configuration which would give the best performance. The first of these studies considers the effect of diode length on internal ohmic losses. These results combined with the effect of diode length on the gross power output yield the net power output as a function of diode length.

To minimize shield weight, net power per unit reactor-core volume must be made as large as possible. The effect on this parameter of diode length, diode diameter, and axial spacing between diodes was then explored.

In addition, the effect of collector thickness on internal ohmic losses and diode weight was studied. The thickness was optimized on a specific-weight basis since the collector thickness of an externally fueled diode can be varied without changing the cell volume for a fixed emitter diameter. After the electrical power aspects of the diode configuration were studied, the effects of fuel thickness on the maximum fuel temperature and core criticality were studied.

In these studies it is assumed that each emitter is isothermal and the current density in each diode is uniform along its length. In reality, the emitter temperature varies along the length of each diode as does the current density. An analysis of diode performance, taking these factors into consideration, is fairly complicated and has recently been presented by Schock. (A. Schock: Analysis and Optimization of "Full-Length" Diodes. Paper presented at the Proceedings of the Second International Conference on Thermionic Electrical Power Generation, Stressa, Italy, May 1968.)

The simplifying assumptions made herein allow hand calculations to be made. They result in an underestimate of ohmic losses in the electrodes and an overestimation of the series lead losses. Although these errors do tend to cancel out, the resulting output power per unit volume may be slightly high for the diode performance maps used. These assumptions have negligible effect on the optimum diode length for this concept using series leads optimized for the isothermal emitter. Shock's work indicates that diode output is very insensitive to series lead configuration. Therefore, the optimized length, when axial

temperature and current densities are taken into account, should not be much different from that presented herein.

Internal Ohmic Losses

Regardless of concept, diodes must be connected in series to build up the voltage to a usable level. Current flowing through a diode results in I^2R losses in the emitter, the collector, and the series lead. The presence of the series lead (see fig. 4) affects the performance of the diode in two ways: (1) The heat it conducts from the emitter to the collector reduces the ΔT between the two electrodes, causing a degradation of performance; and (2) the I^2R loss reduces the overall diode efficiency. Varying the geometry of the series lead in an attempt to reduce the heat transfer causes an increase in the I^2R loss. However, it has been determined (ref. 6) that the optimum series-lead dimensions for maximum net power output are given by

$$\left(\frac{a}{L}\right)_l = JA_e\left[\frac{\rho_l}{\eta k_l(T_e - T_c)}\right]^{1/2}\left(1 - \frac{\eta}{2}\right)^{1/2} \tag{1}$$

(Symbols are defined in appendix A.)

Since diode efficiencies η are of the order of 10 percent, the last term, in parentheses, on the right side of equation (1) can be dropped. Then, after rearranging, equation (1) becomes

$$\left(\frac{L}{a}\right)_l \approx \frac{1}{JA_e}\left[\frac{\eta k_l(T_e - T_c)}{\rho_l}\right]^{1/2} \tag{2}$$

Since $I = JA_e$ and $R = \rho(L/a)$, the I^2R loss for the series lead becomes

$$P_{L,l} = I\left[\rho_l \eta k_l(T_e - T_c)\right]^{1/2} \tag{3}$$

Because electrons are driven from the surface of the emitter to the collector, the current flow varies along the length of the electrodes. This complicates the calculation of the I^2R losses through the electrodes. If a conductor is in parallel with one of the electrodes, an additional problem arises because the current flow through the parallel conductor (fuel cladding) is constant, while the current flow through the electrode

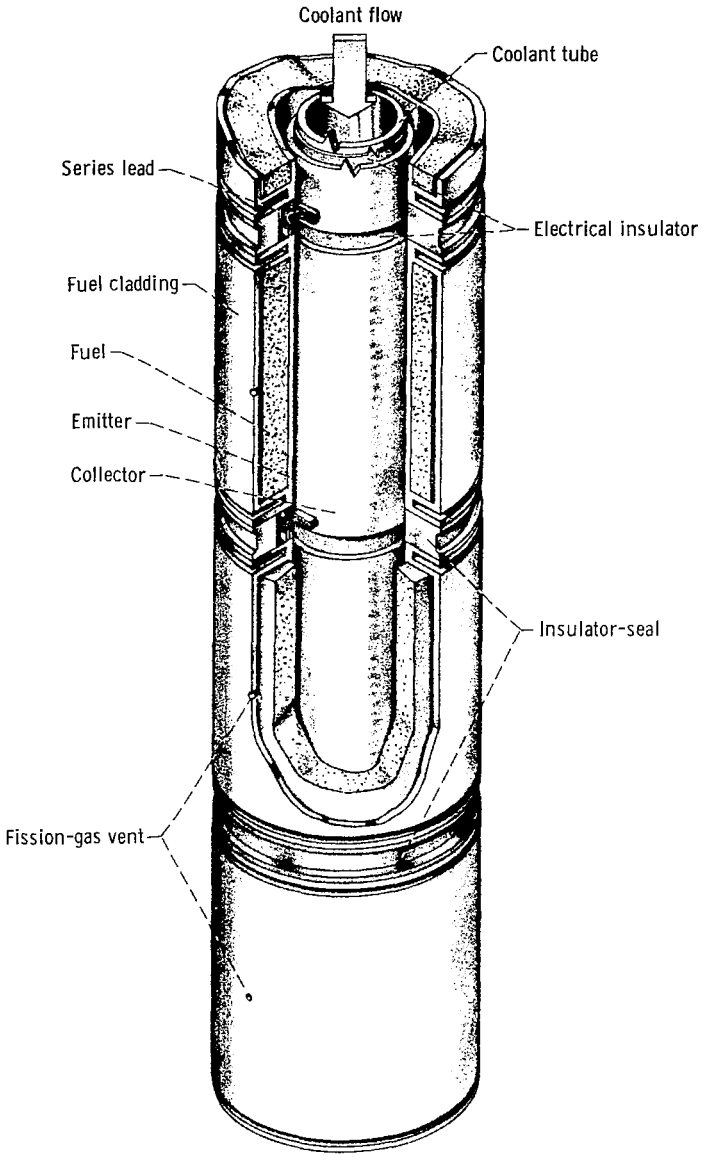

Figure 4. - Fuel element containing externally fueled diodes.

(emitter) varies. A discussion of this problem is given in appendix B where the equations leading to equation (4) are derived. Equation (4) is the summation of the I^2R losses through the emitter (including the fuel cladding) and the collector.

$$P_{L,e} + P_{L,c} = \frac{I^2 L_e}{3}\left(\frac{\rho_e F}{a_e} + \frac{\rho_c}{a_c}\right) \tag{4}$$

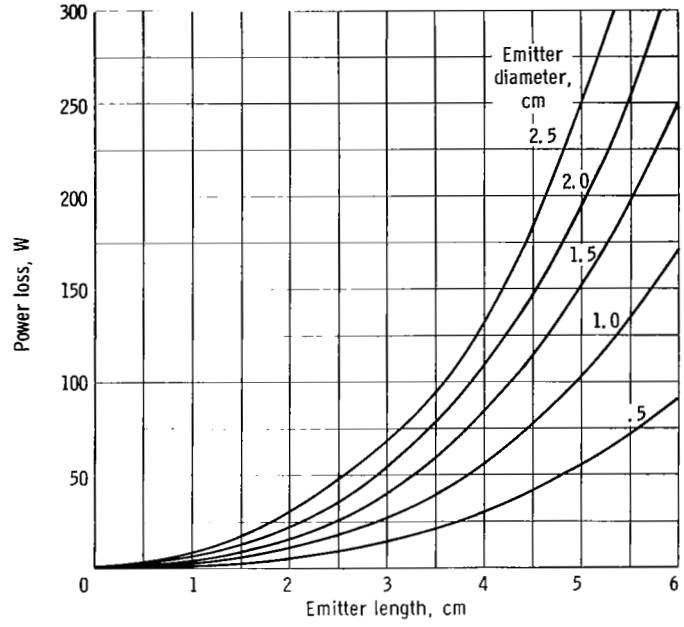

Figure 5. - Total ohmic power loss per diode as function of emitter length and diameter. Loss includes optimum series-lead loss; emitter and cladding areas assumed to be equal; emitter and collector thicknesses, 0.051 centimeter each; current density, 15 amperes per square centimeter.

Combining equations (3) and (4) and substituting $I = JA_e = \pi JD_eL_e$ into the resulting equation give the total ohmic loss for a diode:

$$P_{L,\,tot} = \frac{\pi^2 J^2 D_e^2 L_e^3}{3}\left(\frac{\rho_e F}{a_e} + \frac{\rho_c}{a_c}\right) + \pi J D_e L_e\left[\eta\rho_l k_l (T_e - T_c)\right]^{1/2} \qquad (5)$$

For these studies the electrical conductivity of the fuel was neglected, and the emitter and cladding cross-sectional areas were assumed to be the same for equal thicknesses. By the use of equation (5), power losses as a function of emitter length were computed for a range of emitter diameters from 0.5 to 2.5 centimeters (0.20 to 0.98 in.). The results presented in figure 5 are for assumed emitter and collector thicknesses of 0.051 centimeter (0.020 in.) each. It is evident from figure 5 that the I^2R losses increase rapidly with emitter length. This rapid increase is caused by the L_e^3 term in equation (5) and emphasizes the desirability of keeping emitter lengths short.

Diode Power Output

The gross power output of a diode is a function of emitter surface area, thermal

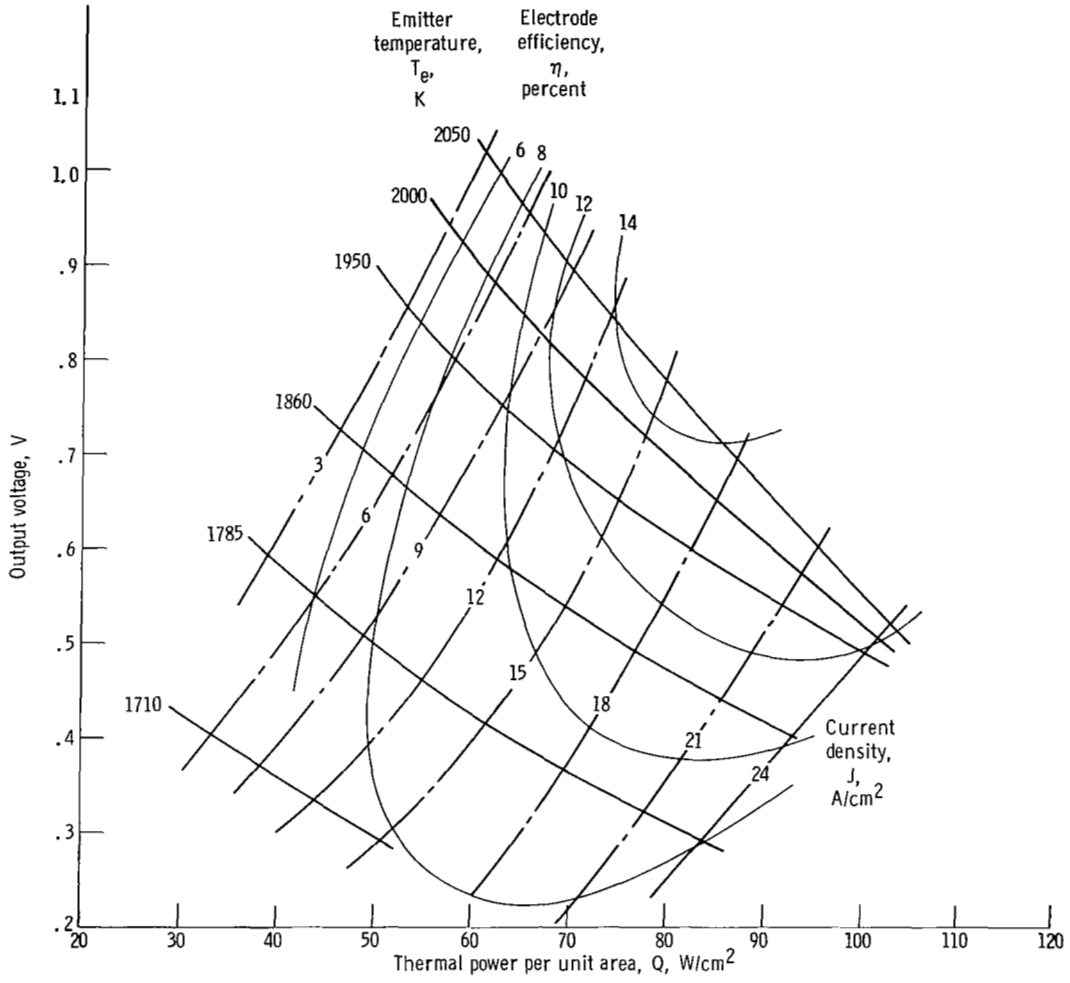

Figure 6. - Thermionic performance as a function of power input.

power input, electrode materials, electrode temperatures, interelectrode gap, and cesium temperature. Experimental data from a laboratory-type diode can be used to construct a diode performance map for a variety of conditions. A typical diode performance map, based on data from reference 7, is shown in figure 6. Although the data were obtained for a different collector material, interelectrode gap, and collector temperature than those of the reference design, they were the best available at the time this study was undertaken. The data were corrected to a collector temperature of 1400 K which was considered to be an upper limit for thermionic diodes. This is a conservative selection because a reduction in the collector temperature would improve the diode performance.

For the core power variation listed in table I the average thermal power input for a diode is about 68.5 watts per square centimeter. This power input and the maximum design current density of 15 amperes per square centimeter result in an average diode volt-

age of about 0.52 volt (see fig. 6). The average gross power output for a diode is then

$$\overline{P}_G = vJA_e$$

$$= 7.8\ \pi D_e L_e (\text{watts}) \tag{6}$$

To determine the usable power per diode, the ohmic losses (fig. 5) are subtracted from the gross power outputs obtained from equation (6). The resulting average net power outputs are then used to determine the maximum power output per unit cell volume.

Emitter Length

A trial-and-error procedure is suggested by the problem of trying to establish the optimum diode dimensions before the critical fuel volume fraction is determined. The critical fuel volume fraction depends on the reactor core size, which cannot be determined without knowing the diode dimensions and the number of diodes needed to produce

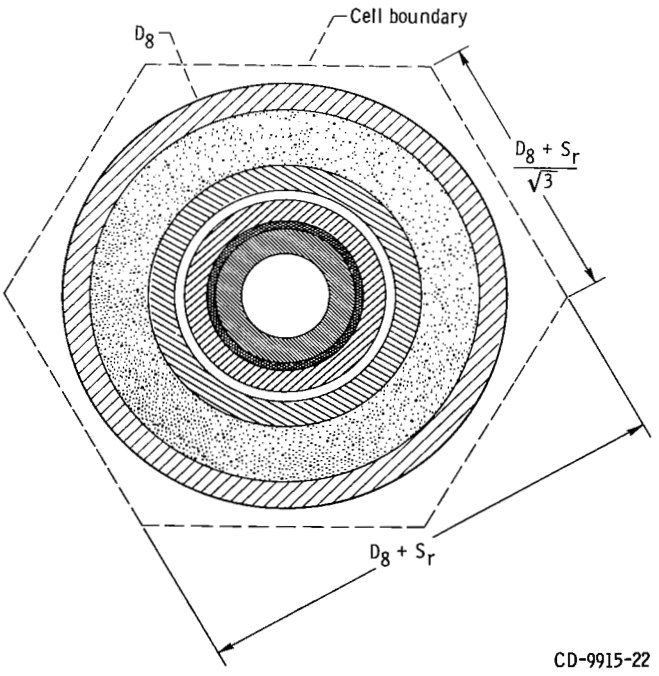

Figure 7. - Diode cell cross section.

a given total power. However, it was discovered that the emitter length of the reference-design diode can be reliably optimized before core size, power level, or criticality are determined.

If it is assumed that the diodes are spaced on an equilateral triangular pitch, the cell cross-sectional area is the hexagonal area shown in figure 7 and is given by

$$a_{cell} = \frac{\sqrt{3}}{2}\left(D_8 + S_r\right)^2 \tag{7}$$

Then, the cell volume is

$$V_{cell} = (a_{cell})(L_{cell})$$

$$= \frac{\sqrt{3}}{2}\left(D_8 + S_r\right)^2(L_e + S_x) \tag{8}$$

where S_r is the radial spacing between fuel elements and S_x is the axial spacing between diodes.

The value of D_8 (the outside diameter of the fuel cladding) in equation (8) depends on the fuel volume. If the fuel volume is neglected, then D_8 equals the emitter diameter plus twice the fuel-cladding thickness. Figure 8(a) shows the effect of diode length (for several emitter diameters) on power per unit cell volume when the fuel is omitted from the cell volume. After the fuel thickness for each emitter diameter was determined from criticality considerations, the calculations were repeated to reflect the true cell volumes. These results are presented in figure 8(b). In all cases the emitter, cladding, and collector thicknesses were each 0.051 centimeter (0.020 in.). The axial and radial spacings were constant at 0.635 centimeter (0.25 in.) and 0.076 centimeter (0.030 in.), respectively. The conservative and simplifying assumption of equal cross-sectional areas for the emitter and the cladding was used throughout in determining the internal ohmic losses.

A comparison of figures 8(a) and (b) shows that the optimum emitter length is not greatly affected by taking into account the change of cell volume due to fuel thickness. The curves also indicate that the optimum emitter length is fairly insensitive to emitter diameter. Values vary over the narrow range of 1.75 to 2.00 centimeters (0.69 to 0.79 in.) for the 5 to 1 range of emitter diameters investigated. Furthermore, for the larger emitter diameters in the region near the optimum length, the power per unit cell volume is relatively insensitive to emitter length also. For example, the power parameter decreases only 5 percent for an increase in length from the optimum of 1.9 centimeters (0.75 in.) to 2.5 centimeters (1.0 in.) for a 1.5-centimeter (0.59-in.) emitter

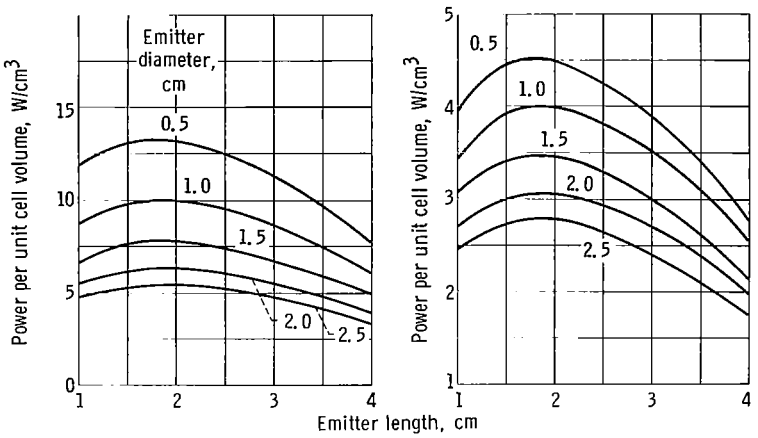

(a) Fuel volume neglected in determining cell volume.

(b) Cell volume includes criticality determined fuel volume.

Figure 8. - Effect of diode length and diameter on net power output per unit cell volume. Radial spacing of 0.076 centimeter and axial spacing of 0.635 centimeter between diodes are included in cell volumes.

diameter. Since the penalty is small, it was decided to trade off a slight increase in reactor-core size for a reduction in the number of diodes by selecting the 2.5-centimeter emitter length for the reference-design diode.

Collector Thickness

When the I^2R losses were previously calculated, an arbitrary collector thickness of 0.051 centimeter (0.020 in.) was used. It can be seen from figure 1 (p. 5) that for a given emitter diameter D_5 and interelectrode gap, the collector thickness can be varied without changing the external dimensions of the diode. For a fixed insulator thickness and coolant-tube wall thickness, increasing the collector thickness reduces the coolant flow passage and changes the weight of the diode. But a thicker collector reduces the I^2R loss which increases the net power output per diode and decreases the number of diodes needed to produce a given core power. Increasing the collector thickness is beneficial at least as long as the specific weight of the diode decreases and the pressure drop through the coolant passage does not become excessive. Since this study is restricted to the reactor core, the effect of increased pumping power on the total system weight was not considered.

The effect of varying the collector thickness was based on specific weight rather than on power per unit cell volume because any increase in diode output automatically in-

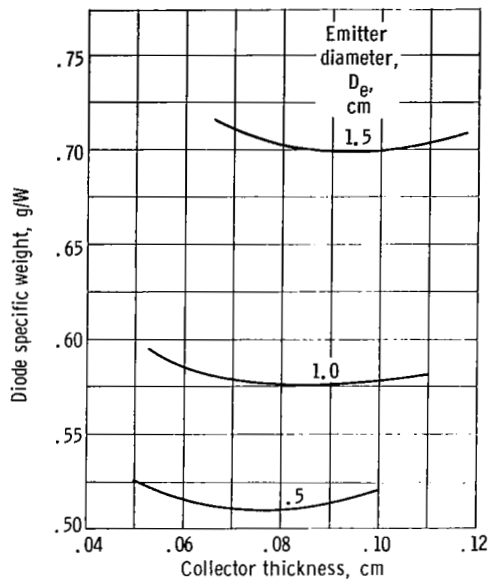

Figure 9. - Diode specific weight as function of collector thickness. Emitter length, 2.5 centimeters; fuel thickness, 0; emitter thickness, 0.051 centimeter; cladding thickness, 0.051 centimeter; insulator thickness, 0.025 centimeter; coolant pipe thickness, 0.102 centimeter.

creases the power per unit cell volume since the cell volume is unchanged. Figure 9 presents the diode specific weight as a function of collector thickness for three emitter diameters and for the reference-design emitter length of 2.5 centimeters (~1.0 in.). For these calculations it was assumed that the coolant-tube wall thickness of 0.102 centimeter (0.040 in.) and the trilayer insulator thickness of 0.025 centimeter (0.010 in.) were constant. The resulting optimum collector thicknesses are 0.076, 0.086, and 0.094 centimeter (0.030, 0.034, and 0.037 in.) for emitter diameters of 0.5, 1.0, and 1.5 centimeters, respectively.

Depending on the relative importance of shield weight it may be desirable to increase the collector thickness above the value resulting in optimum diode specific weight. For a reactor that is not criticality limited, increasing the collector thickness will result in a smaller reactor and lower shield weight. The shield weight decrease would have to be compared with the weight increase of the diodes in order to obtain the minimum reactor weight for a given power level. For a criticality limited reactor, the reactor size reduction would not be as great because the required fuel volume fraction increases with decreasing reactor size. Therefore, the reactor size reduction due to a decrease in the number of diodes is offset somewhat by an increase in the individual diode cell volume.

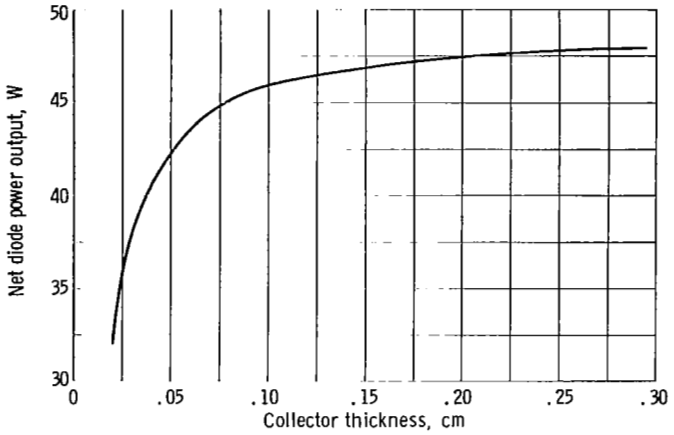

Figure 10. - Net diode power output as function of collector thickness. Emitter diameter, 1.0 centimeter; emitter length, 2.5 centimeters.

Figure 10 shows the effect of varying collector thickness on net power output for a given diode. The curve indicates that for this particular diode, only marginal increases in performance are realized as the thickness increases above 0.10 centimeter (0.039 in.).

Stress calculations were not performed for the given coolant-tube wall thickness; therefore, any reduction in this thickness would allow an additional increase in the collector thickness without increasing the diode weight. This would reduce the collector ohmic losses and the reactor-core size even further.

Fuel Thickness

The maximum fuel thickness must be small enough to prevent excessive fuel temperatures. Figure 11 shows the temperature difference across the UO_2 as a function of fuel thickness for several emitter diameters for the maximum design heat flux. The calculations were made by using equations from reference 8 for an internally cooled cylindrical shell with uniform internal heat generation. For an emitter temperature of 2000 K (3600° R) a wide range of thicknesses can be used before the melting point of UO_2 is reached in normal operation.

The minimum fuel thickness must be large enough to satisfy the criticality requirements. To determine these thicknesses as a function of emitter diameter, criticality curves from reference 9 were used. Given in this reference are plots of fuel volume fraction against reactor-core diameters for several fuels and beryllium oxide (BeO) reflector thicknesses. In order to provide adequate reflector control, a reflector thickness

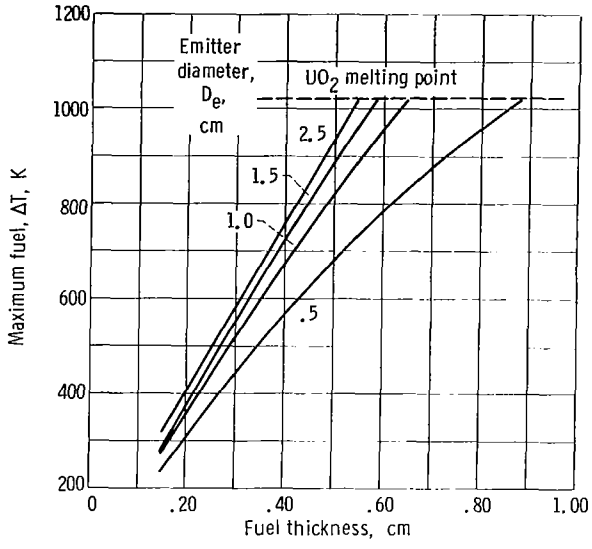

Figure 11. - Maximum fuel temperature difference as function of fuel thickness. Thermal heat flux, 77 watts per square centimeter; emitter temperature, 2000 K.

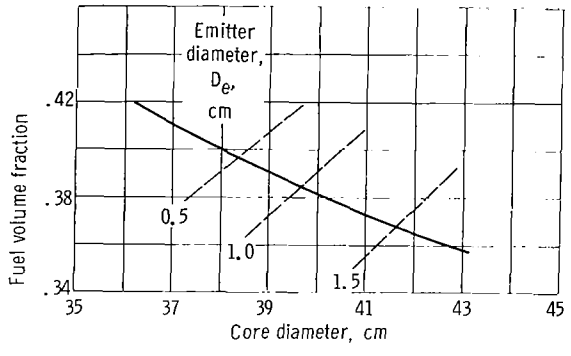

Figure 12. - Determination of critical fuel volume fractions for several emitter diameters. (Solid curve represents data from ref. 9 for UO_2 fuel, effective multiplication factor of 1.05, 10.2-centimeter beryllium oxide reflector, and core length to diameter ratio of 1.)

of 10.2 centimeters (4.0 in.) was chosen. The solid line in figure 12 represents the data from reference 8 for the chosen reflector thickness, fully enriched UO_2 fuel, an effective multiplication factor k_{eff} of 1.05, and a reactor-core length to diameter ratio L/D of 1. These data are for a fast, liquid-metal-cooled reactor. For the materials normally found in the nonnuclear components of such reactors, variation in composition has little effect on the fuel volume fraction requirements. Therefore, the solid curve is adequate for the purpose of determining the critical fuel volume fraction as a function of emitter diameter.

The dashed curves intersecting the solid line in figure 12 determine the critical fuel volume fractions for each of the emitter diameters shown. The dashed curves were obtained in the following manner. The fuel volume fraction is given by

$$F_v = \frac{V_f}{V_{cell}} = \frac{\frac{\pi}{4} L_e \left(D_7^2 - D_6^2\right)}{\frac{\sqrt{3}}{2} \left(D_8 + S_r\right)^2 (L_e + S_x)}$$

$$= \frac{2\pi t_f (D_e + 2t_e + t_f) L_e}{\sqrt{3}\left[D_e + 2(t_e + t_f + t_w) + S_r\right]^2 (L_e + S_x)}$$

or

$$F_v = \frac{2.89\ t_f (D_e + 0.102 + t_f)}{\left(D_e + 2t_f + 0.28\right)^2} \tag{9}$$

when the emitter wall thickness t_e and the fuel cladding thickness t_w are 0.051 centimeter (0.020 in.) each, the radial spacing between fuel elements S_r is 0.076 centimeter (0.030 in.), the axial spacing between diodes S_x is 0.635 centimeter (0.25 in.), and the emitter length L_e is 2.5 centimeters (1.0 in.).

For a reactor-core L/D = 1, the core volume is given by

$$V_{core} = \frac{\pi}{4} D_{core}^3$$

or

$$D_{core} = 1.083\ V_{core}^{1/3} \tag{10}$$

The core volume can also be approximated by

$$V_{core} = \frac{\sqrt{3}}{2} N \left(D_8 + S_r\right)^2 (L_e + S_x)$$

$$= 2.72\ N \left(D_e + 2t_f + 0.28\right)^2\ cm^3 \tag{11}$$

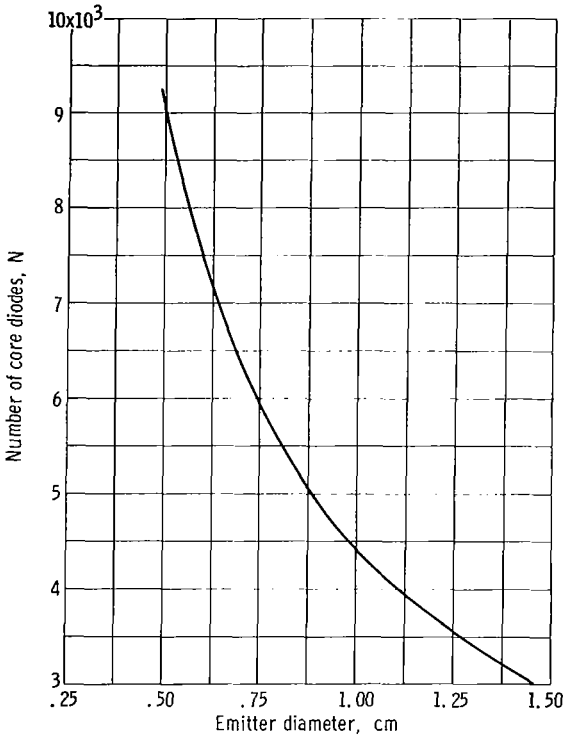

Figure 13. - Number of core diodes as function of emitter diameter for diode-specific-weight-optimized collector thicknesses. Core power, 200 kW electric; emitter length, 2.5 centimeters.

The number of core diodes N is determined by dividing the net reactor power output by the average power output of a diode. Figure 13 shows N plotted against emitter diameter for a 200-kW electric reactor. The calculations were performed for diodes with optimized collector thicknesses and the reference-design emitter length of 2.5 centimeters.

By assigning arbitrary values of fuel thickness t_f for each given emitter diameter D_e and taking N from figure 13, equations (9), (10), and (11) yield the dashed curves of figure 12. The intersections of the dashed curves with the solid curve give the reactor-core diameters and the critical fuel volume fractions. The smallest diode considered results in a 38.3-centimeter-diameter (15.0-in.-diam) reactor core while the largest results in a 41.6-centimeter-diameter (16.4-in.-diam) reactor core. These dimensions are minimal since no allowance was made for fuel zoning.

The critical fuel volume fractions from figure 12 were substituted back into equation (9) to obtain the minimum fuel thicknesses. These thicknesses, which vary from 0.28 to 0.445 centimeter (0.11 to 0.175 in.) for emitter diameters of 0.5 to 1.50 centimeters (0.197 to 0.591 in.), are shown in figure 14.

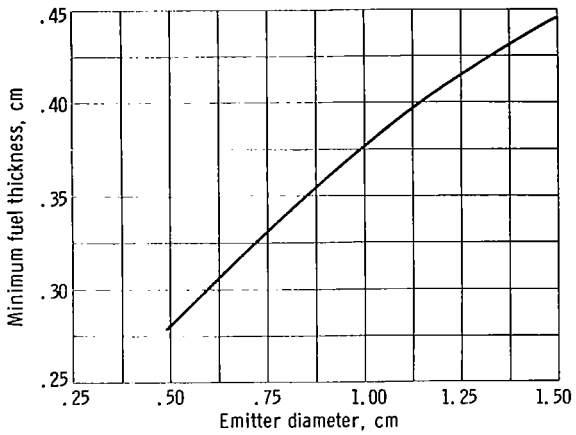

Figure 14. - Critical (minimum) fuel thickness as function of emitter diameter based on data from reference 9 for UO_2 fuel, effective multiplication factor of 1.05, 10.2-centimeter beryllium oxide reflector; core length to diameter ratio of 1.

Emitter Diameter

The preceding studies have shown that the emitter diameter should be kept as small as possible in order to obtain the maximum power output per unit of cell (or reactor core) volume. However, as the emitter diameter decreases the number of diodes needed to produce a given power level increases rapidly, as shown in figure 13. Small sizes and large quantities of diodes complicate fabrication, assembly, and testing problems. For these reasons it is desirable to select as large an emitter diameter as possible without paying an unreasonable reactor size penalty.

The reactor size penalty resulting from using emitter diameters larger than 0.5 centimeter (0.2 in.) is more severe for a high-power reactor than it is for a criticality limited reactor. This difference results from the effect fuel thickness has on the cell volume for a given emitter diameter. This effect is illustrated in figure 15 where the maximum values of power per unit cell volume obtained from figures 8(a) and (b) are plotted against emitter diameter. When the criticality determined fuel volume in included in the cell volume, the curve is fairly flat, as shown by the lower curve. As reactor-core size increases, the fuel volume per cell decreases and the upper curve of figure 15 is approached. The steeper slope of the upper curve indicates a greater power penalty for high-power reactors as the emitter diameter increased beyond 0.5 centimeter.

There is an upper limit on the emitter diameter for the reference design. This limit is determined by the maximum fuel temperature reached after an open-circuit failure. It is shown in the section Open-Circuit Temperature Rise that this diameter is 1.30 centimeters (0.51 in.) for the reference-design diode with the criticality deter-

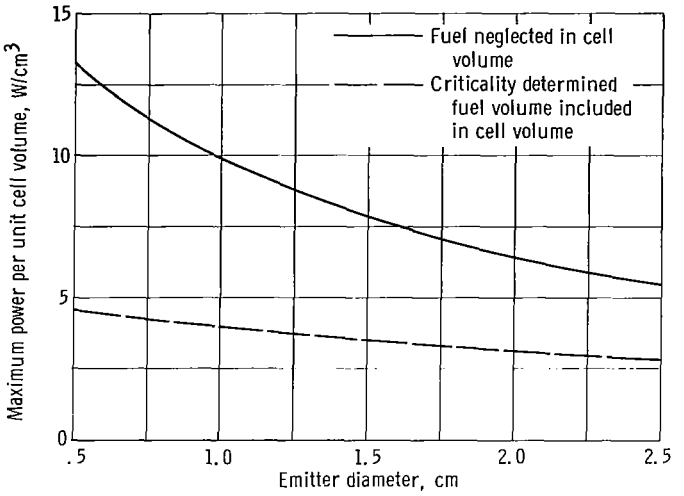

Figure 15. - Maximum power per unit cell volume as function of emitter diameter.

mined fuel thicknesses shown in figure 14. Therefore, based on the above considerations, an emitter diameter of 1.25 centimeters (0.49 in.) was selected for the reference-design diode.

Spacings Between Diodes

In the calculations of power per unit cell volume, the axial and radial spacings between diodes were held constant at 0.635 and 0.076 centimeter (0.25 and 0.030 in.), respectively. Those dimensions were arbitrarily selected as the smallest practical from manufacturing and assembly considerations. However, varying the axial spacing causes the optimum emitter length and the maximum power per unit cell volume to vary. If it were possible to have no axial space between diodes, the power per unit cell volume would vary with emitter length, as shown by the upper curve of figure 16. When axial spacing is included in the cell volume, the power per unit cell volume versus emitter length passes through a maximum point, as shown by the lower curve of figure 16. The reason is that a fixed axial spacing dimension contributes more volume (in percent) to the cell volume for a small emitter length than it does for a large emitter length. As the emitter length increases, the contribution of the spacing to the total cell volume decreases, and the curve approaches the curve of zero axial spacing. The loss of power per unit cell volume as indicated by the difference between the two curves emphasizes the need to keep the axial spacing as small as possible. Radial spacing has the same effect that the fuel thickness has on the power per unit cell volume (fig. 15). Therefore, it should also be kept as small as possible.

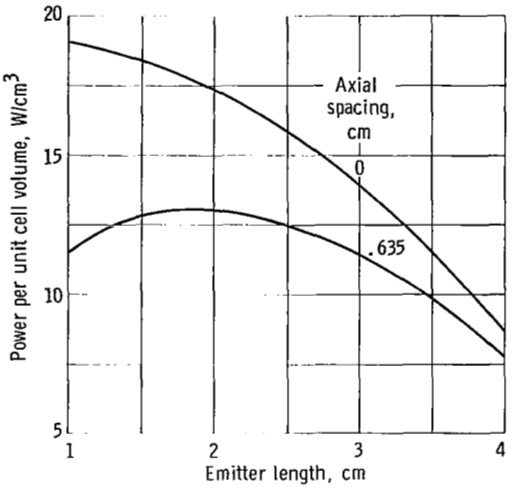

Figure 16. - Effect of axial spacing on diode power per unit cell volume. Radial spacing, 0.076 centimeter; emitter diameter, 0.5 centimeter; fuel volume neglected.

REFERENCE DESIGN

Fluid Flow Analysis

The preceding studies established the dimensions of the reference-design diode. Several diodes are stacked one upon the other and series connected to form a fuel element which must be analyzed for pressure drops to assure that the basic dimensions are satisfactory. The approximate core length, from figure 12 where core L/D = 1, is about 40.5 centimeters (15.9 in.). Then, the number of diodes in a fuel element is given approximately by

$$n = \frac{L_{core}}{L_e + S_x} = 12.9$$

Therefore, 13 diodes should be used. When about 5 centimeters (1.97 in.) are allowed for cesium chambers and expansion joints, the core length becomes 45.7 centimeters (18.0 in.)

If it is assumed that the maximum allowable temperature rise of the lithium coolant as it passes through a fuel element is 55 K (100° R), the corresponding minimum weight flow is

$$w = \frac{n\bar{Q}A_e}{C_p \Delta T} = 0.036 \text{ kg/sec } (0.079 \text{ lb/sec})$$

The Reynolds number for the lithium coolant flowing through the fuel element is

$$N_{Re} = \frac{wD_1}{\mu a_1} = 21\,900$$

and the friction factor for that N_{Re} is $f = 0.025$. Neglecting entrance and exit losses, the coolant pressure drop through a fuel element is

$$\Delta p \approx \frac{fw^2 L_{core}}{2\rho'_g D_1 a_1^2}$$

which is well below the total head available from a typical electromagnetic pump for a system of this size (ref. 10). Therefore, the coolant flow rate could be increased considerably without having an excessive pressure loss with an emitter of this size, or a smaller coolant flow passage (and emitter diameter) could be tolerated with the given coolant flow rate.

Electrical Zoning

If no effort is made to match electric conversion with the reactor-core thermal power distribution, high losses in power output will be incurred (ref. 2). Many methods have been proposed to reduce the effects of varying power throughout the reactor core. Some of these methods attack the problem at the heat source; that is, fuel zoning and/or the introduction of moderator material in zones are used to give heat fluxes which lead to more uniform emitter temperatures throughout the reactor core (ref. 1). Other methods that have been suggested include varying the diode geometry to match the thermal power input. Examples of studies on variable emitter length and on variable fuel loading (for a constant emitter length) are presented in reference 2. Also, combinations of two or more methods could be employed in the same reactor core.

For the reference design it was assumed that the reactor-core thermal power was first flattened by nuclear means to a peak-to-minimum power ratio of 1.2. Then, the effect of the resulting radial thermal power variation was reduced by employing electri-

cal zoning. Basically, electrical zoning is an attempt to keep all series-connected diodes of a given circuit in as uniform a thermal power region as possible. The degradation of performance of series strings of diodes in a nonuniform thermal power region is best illustrated by means of the diode performance map (fig. 6).

Since all the reference-design diodes are the same size, the constant current density J lines of figure 6 are, in effect, constant current lines. It is shown in the figure that for any given constant current density the voltage decreases as the input power decreases. If all the core diodes operate at a constant current density, there is no way to avoid losing electrical power (for diodes of the same size) as the input power decreases. Electrical zoning (varying current density from zone to zone) provides a means of recovering some of this lost power. The highest-powered diodes of a given zone are operated at a current density that results in the maximum net power output without exceeding the maximum allowable emitter temperature. The determination of this optimum operating curve is given in the following paragraphs.

The maximum gross power output for a given thermal power input can be determined from figure 6 (p. 14). The gross electrical power outputs for several values of thermal input power are plotted against current density in figure 17. The electrical power output maximizes for a particular value of current density. However, it is the net power output that is important, so the gross power output has to be reduced to account for the internal I^2R losses.

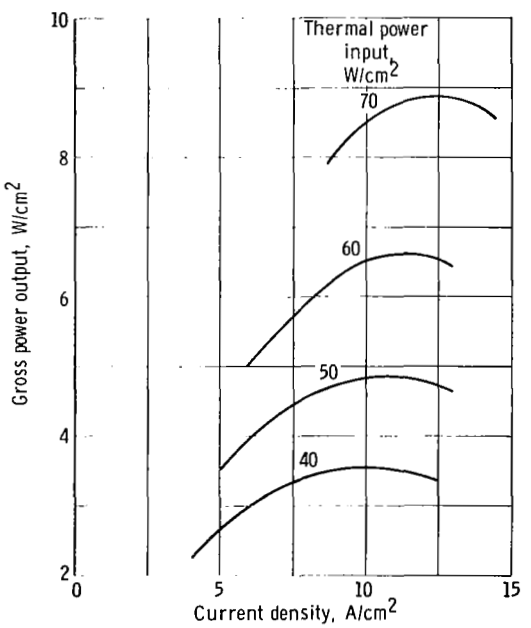

Figure 17. - Diode gross power output as function of current density for several values of constant thermal power input (based on data from fig. 6).

The I^2R losses shown in figure 5 (p. 13) were calculated for a constant current density of 15 amperes per square centimeter and for a nonoptimum collector thickness. For this study the losses were recalculated by using the dimensions of the reference-design diode. The increase in cladding cross-sectional area due to fuel thickness was neglected; therefore, the values of the I^2R losses shown in figure 18 for varying current density are slightly conservative. These losses, when subtracted from the gross electrical power output values shown in figure 17, give the net electrical power outputs.

Net electrical power output plotted against current density results in curves similar to those of figure 17. The resulting values of maximum net power output are plotted against thermal power input in figure 19 to show the effect of increasing input thermal

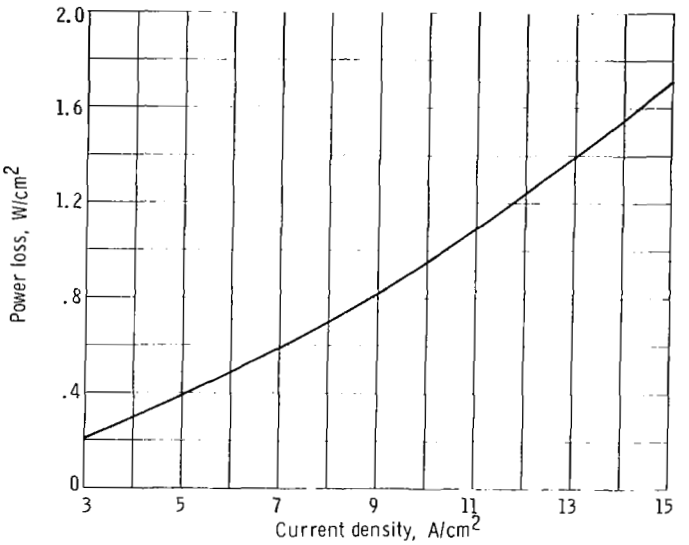

Figure 18. - Total ohmic losses for reference-design diode including optimum series lead. (Cladding and emitter cross-sectional areas are assumed to be equal.)

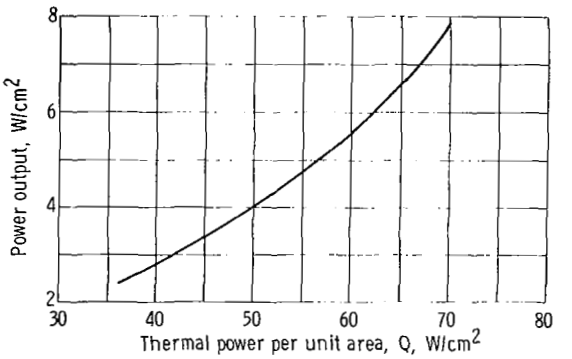

Figure 19. - Maximum net electrical power output for reference-design diode as function of thermal power input.

power on diode performance. This information is used, along with the appropriate values of current density, to establish the optimum operating line for the reference diode.

Voltage values for each pair of maximum net electrical power and current density values can be readily determined. These voltages and the corresponding values of thermal input power yield the maximum net power output operating line (heavy-dashed curve) in figure 20. The curve intersects the $T_e = 2000$ K curve at a thermal power input of about 71 watts per square centimeter. Since this is the maximum allowable emitter temperature, any diode with a thermal power input greater than 71 watts per square centimeter is limited by the $T_e = 2000$ K line. These two curves (the $T_e = 2000$ K line and the maximum net power output line) establish the operating points of the highest-powered diodes of each zone in the following studies.

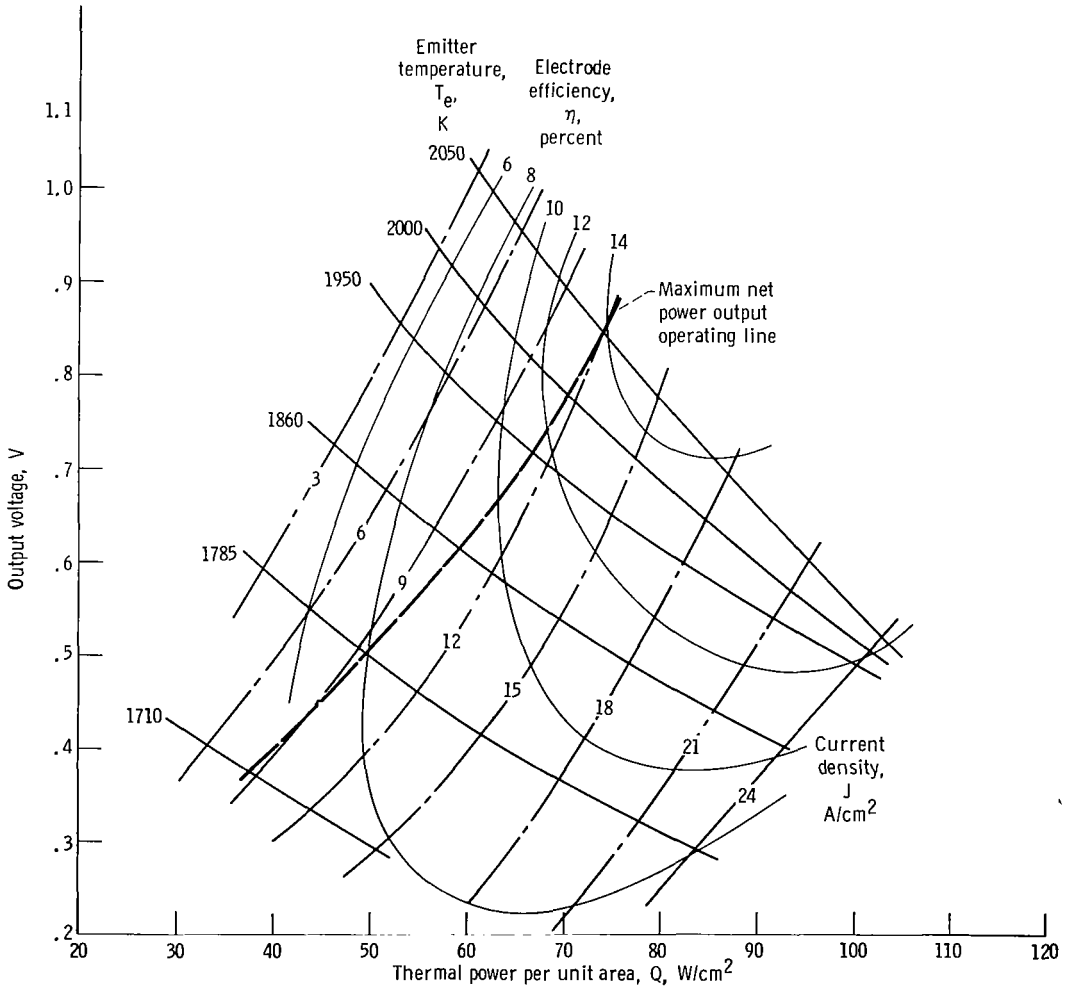

Figure 20. - Performance map indicating optimum operating curve for reference-design diode.

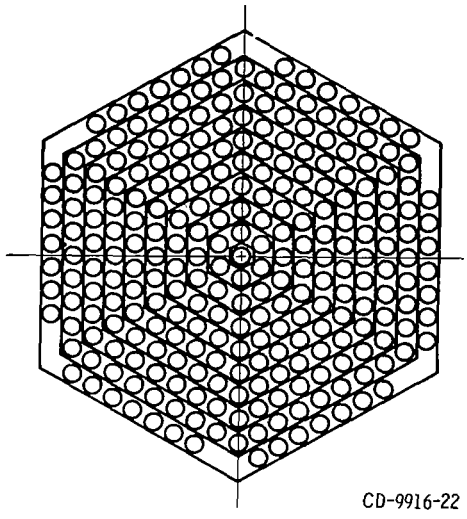

Figure 21. - Ten-ring core model.

The core was divided into 10 rings of fuel elements, as shown in figure 21. Ring 1 is the central ring (actually one fuel element), and the outer ring is ring 10. Four cases, each with different electrical zoning, were studied and then compared with an ideal case (case 5) where it was assumed that the radial core power was uniform. The following assumptions were used:

(1) The performance of each diode is determined by the map shown in figure 20.

(2) Radial and axial power variations are as indicated in table I (p. 4) (except for case 5 which has uniform radial power).

(3) The maximum power density is 77 watts per square centimeter.

(4) The maximum emitter temperature is 2000 K.

(5) All the fuel elements in a given zone are series connected.

(6) All the fuel elements in a given ring have the same thermal input power.

The cases are briefly described as follows:

Case 1. - All the fuel elements are series connected to form a one-zone core. The current density is 15 amperes per square centimeter, which corresponds to a thermal power input of 77 watts per square centimeter and an emitter temperature of 2000 K (fig. 20).

Case 2. - This is a two-zone core. Zone 1 contains rings 1 to 7, and zone 2 contains rings 8 to 10 (see fig. 21). The current density in zone 1 is 15 amperes per square centimeter. The highest-powered diodes of zone 2 have a heat input of 70.1 watts per square centimeter. This thermal power input and the maximum net power output curve of figure 20 result in a current density of about 11.5 amperes per square centimeter for zone 2. The operating points of the highest-powered diodes in each zone are illustrated in figure 22. It can be determined by using values taken from the figure that the highest-

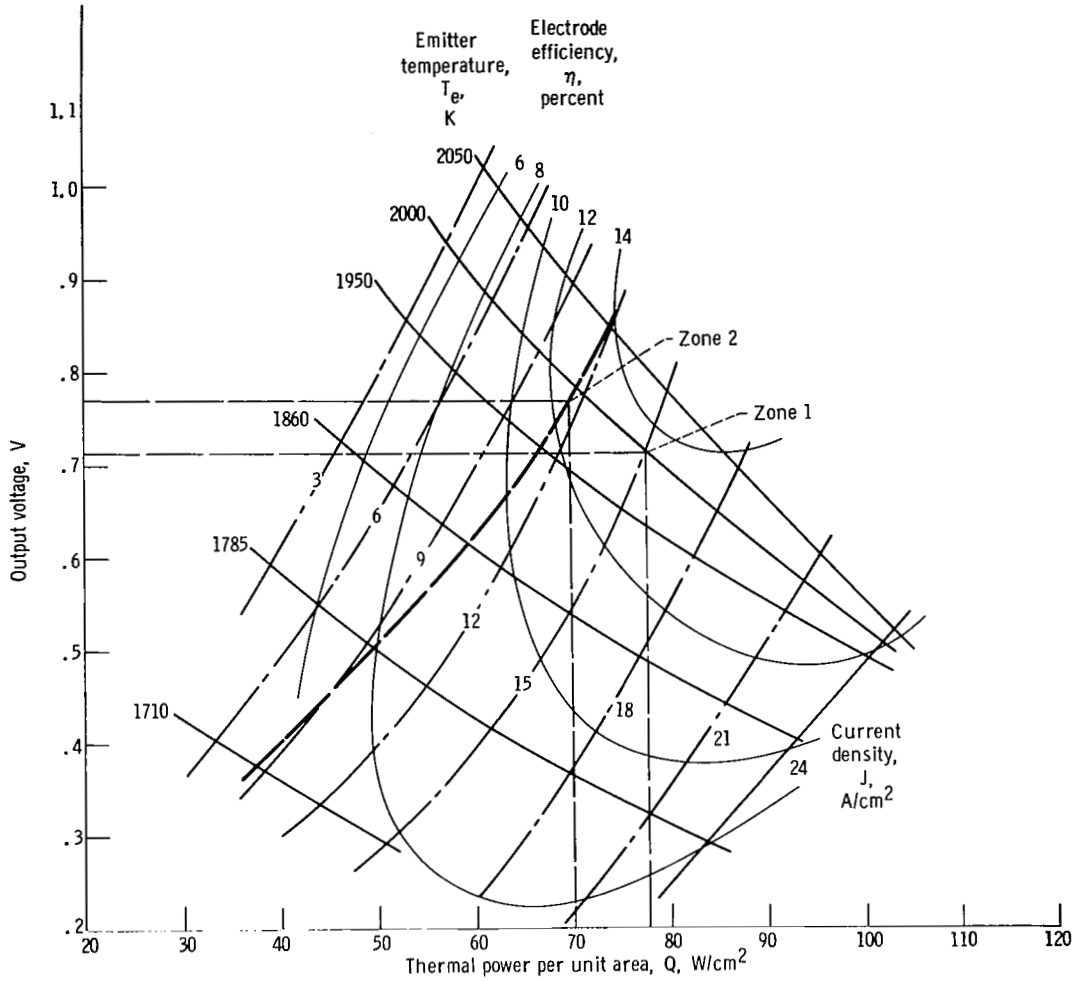

Figure 22. - Operating points of highest-powered diodes of each zone for case 2.

powered diode in zone 2 produces about 8.9 watts per square centimeter. That same diode operating in case 1 on the J = 15 amperes per square centimeter line produced 8.1 watts per square centimeter or almost 10 percent less power.

Case 3. - This is a four-zone case where zones 1 to 4 are composed of rings 1 to 4, 5 and 6, 7 and 8, and 9 and 10, respectively. The analytic procedure is an extension of that described for case 2. That is, each zone shifts to a new J-line limited only by the maximum emitter temperature of 2000 K or the maximum net power output line.

Case 4. - This is the limiting case as far as the number of zones is concerned. Here, each ring is a separate electrical zone whose current is dictated by the highest-powered diode of that ring.

Case 5. - This is the ideal case where the radial power is assumed to be uniform across the core. However, the axial power varies the same as in all the previous cases.

In effect, this case can be thought of as a core composed entirely of ring 1 fuel elements.

The results of this study are presented in table II. As more zones are introduced there is an additional gain in net core power output. Part of the gain is caused by reduced I^2R losses which result from zones operating with current densities less than the maximum of 15 amperes per square centimeter.

The radial power variation assumed in table I (p. 4) results in a loss of power of about 25 percent (comparison of case 1 with case 5). About half of this power can be recovered by using only four zones (case 3). The slight increase in net power output obtained by using 10 zones (case 4) is marginal and does not justify the increased electrical complexity compared with a four-zone case. Therefore, case 3 was used as the model for the reference design.

TABLE II. - SUMMARY OF ELECTRICAL ZONING STUDY

Case	Zone	Ring	Zone voltage, V	Current density, J, A/cm^2	Maximum diode current, I, A	Gross power, kW electric	I^2R loss, kW electric	Net core power, kW electric	Core power relative to case 5
1	1	1 to 10	1633	15.0	147	240.0	56.6	183.4	0.753
2	1	1 to 7	892	15.0	147	131.1	27.7	203.2	0.835
	2	8 to 10	1057	11.5	113	119.4	19.6		
3	1	1 to 4	275	15.0	147	40.4	8.1	215.8	0.886
	2	5, 6	451	13.2	133	60.0	9.7		
	3	7, 8	686	12.0	118	80.9	12.3		
	4	9, 10	714	11.0	108	77.1	12.5		
4	1	1	8	15.0	147	1.2	0.2	218.1	0.896
	2	2	49	14.5	142	6.9	1.2		
	3	3	100	14.1	138	13.7	2.4		
	4	4	151	13.8	135	20.4	3.4		
	5	5	205	13.2	130	26.6	4.3		
	6	6	260	12.8	126	32.7	5.2		
	7	7	324	12.0	118	38.2	5.7		
	8	8	374	11.5	113	42.2	6.2		
	9	9	400	11.0	108	43.1	6.7		
	10	10	324	10.7	105	34.0	5.6		
[a]5	1	1 to 10	2046	15.0	147	300.0	56.6	243.4	1.000

[a]Case 5 has flat radial power distribution.

Electrical Circuits

Each core-length fuel element contains 13 diodes which are connected in series electrically. In order to reduce the power loss caused by an open circuit, three fuel elements are joined together in parallel electrically. Several of these "trielements" are connected in series to produce the desired circuit voltage.

The electrical zoning study indicated that a reactor core with four zones would be the best practical arrangement for the reference design. Figure 23 shows a schematic cross section of the core with the zones indicated by the heavy lines. Each zone contains the number of circuits indicated in table III where zone 1 is the central zone. Multiple circuits are used to limit any one circuit to 100 volts or less to prevent a trilayer insu-

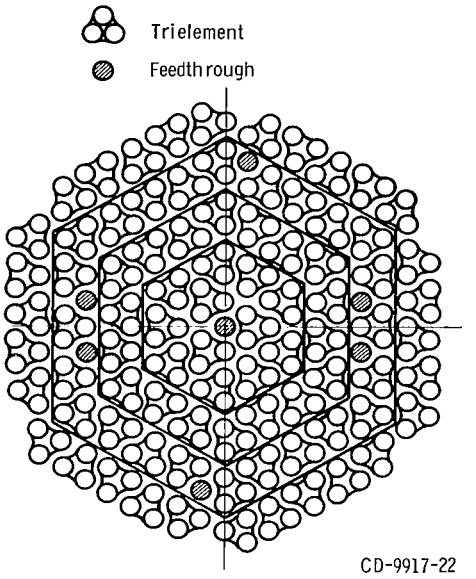

Figure 23. - Schematic of reference-design core showing trielements grouped into four electrical zones.

TABLE III. - ELECTRIC CIRCUITS BY ZONES

Zone	Trielements per zone	Circuits per zone	Approximate circuit voltage, V	Approximate circuit current, A	Approximate circuit power, kW electric	Approximate zone power, kW electric
1	12	1	71	441	31.3	31.3
2	18	2	63	400	25.1	50.2
3	24	2	88	354	31.1	62.2
4	30	2	100	324	32.4	64.8

lation breakdown. Since both circuits of each multiple-circuit zone are paralleled to one set of power conditioning equipment, a total of four sets of power conditioning equipment is required for the reference-design reactor.

The approximate currents and voltages listed in table III are based on the results obtained for case 3 of the electrical zoning study. However, the case 3 values were determined for series-connected fuel elements and not for series-connected trielements. Therefore, the voltages and currents had to be adjusted to account for the series-parallel networks created by the use of trielements. In addition, the power lost by removal of fuel elements for feedthrough positions (the shaded circular areas of fig. 23) was taken into account. When trielements are arranged as shown in figure 23, it is impossible for all three fuel elements to be in the same ring and have the same input power. Therefore, there will be a slight voltage mismatch when they are paralleled, causing additional losses which are not accounted for in table III.

Arrangement of Components

A simplified sketch of the core illustrating the main components (except for individual diodes) is shown in figure 24. The modular power package is the trielement. All the trielements are identical, but those labeled A are oriented upside down with respect to the B trielements. This simplifies the series electrical connections between trielements and keeps the connectors short. Although parallel cross connections between adjacent diodes are not shown, the reference design premits such interconnections if there is an advantage in doing so.

From the inlet nozzle the liquid-metal coolant is distributed throughout the reactor core by means of a plenum. The lithium flows through the centers of the fuel elements and through the passage formed by the double walls of the containment vessel. This cools the collectors, the containment vessel, and the reflector. Insulation must be installed between the inner wall of the containment vessel and the outer ring of trielements. If this is not done, the outer ring of trielements will lose too much heat, degrading the performance of electric zone four. Radiation shields are used for this purpose in the reference design.

The high-voltage leads are limited to one per electrical circuit. The opposite end of each electrical circuit is grounded to the liquid-metal-coolant plenum. In order to use the electric power developed, one side of a load must be connected to the high-voltage lead while the other side must be grounded to the liquid-metal-loop piping outside the reactor core.

Fission gases are collected in the void space surrounding the fuel elements. The pressure buildup in the containment vessel is controlled by removing the excess gases

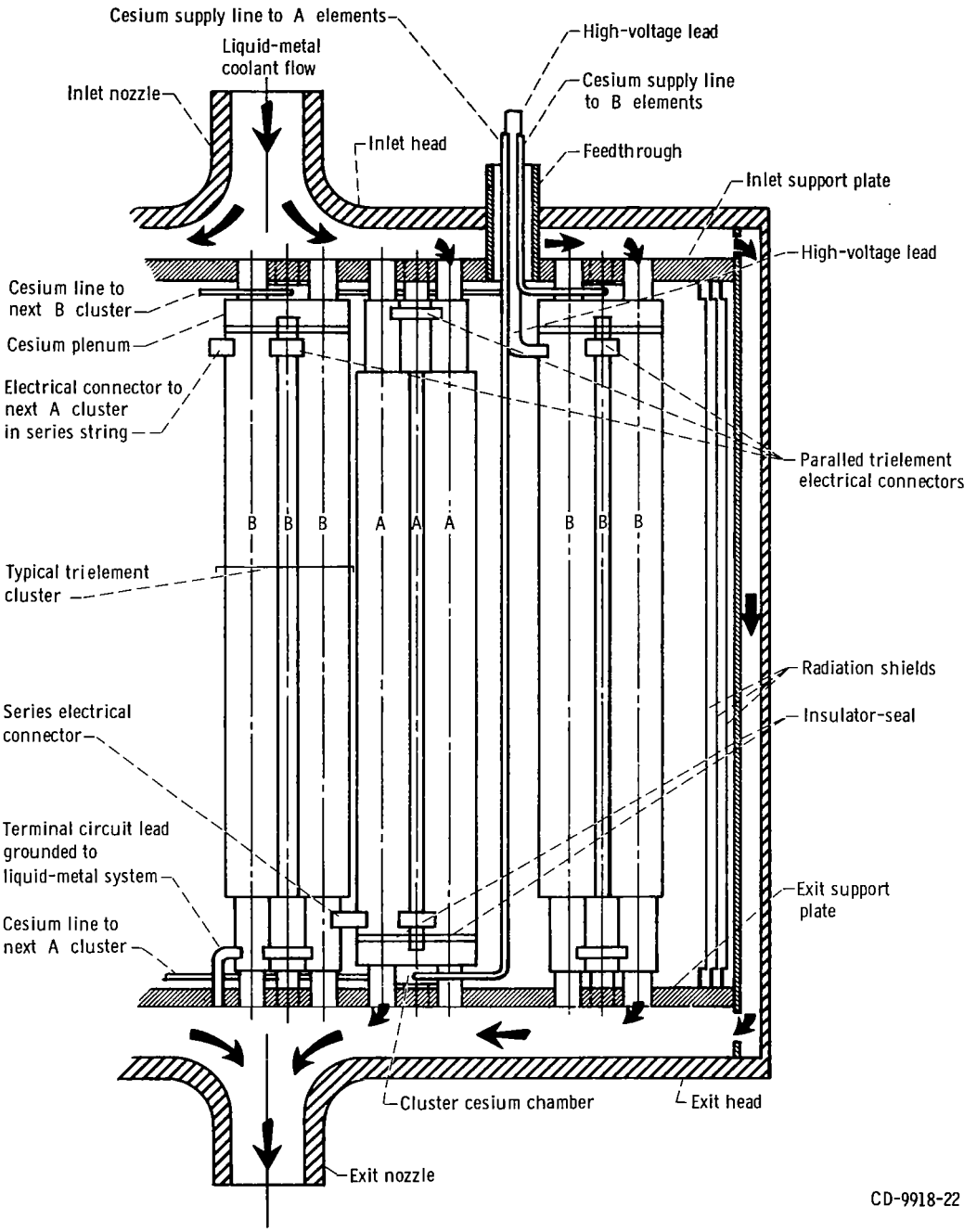

Figure 24. - Core assembly of 200-kilowatt electric thermionic reactor.

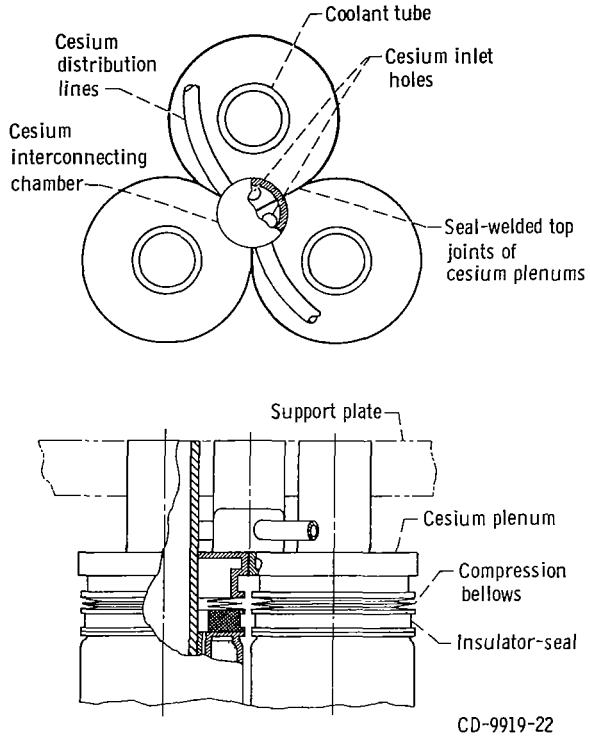

Figure 25. - Trielement details.

from the vessel by means of a tube welded into one of the feedthroughs. If the gases can not be discharged directly to space, some other method of controlling the pressure will have to be devised. One method might be to pump the gases to a high-pressure shielded retention tank located outside the containment vessel.

The three fuel elements that form a trielement are joined together by means of a common cesium plenum. For each electrical circuit there are two cesium supply lines (from a reservoir located outside the containment vessel) that are brought into the reactor core through a feedthrough. One line supplies cesium to an A trielement while the other supplies a B trielement. The cesium is distributed to the rest of the trielements in the string by short lines that interconnect plenums. Details of the cesium-plenum end of a trielement are shown in figure 25.

Seal Designs

In a vented-fuel diode design it is necessary to contain the cesium in the interelectrode space, and it is desirable to keep the fission gases out. Some seals in a thermionic system have to be electrical insulators because they may be in intimate contact with

an emitter and a collector, two adjacent emitters, or two adjacent collectors depending on the particular design and type of diode. Stress problems associated with ceramic insulator-seals are extensively analyzed in reference 11. This section analyzes the problems in the metallic components of two different types of sealing arrangements for the reference design. Although both radial and axial differential thermal expansions have to be considered, only the axial effects were considered for the two designs which are described in the following paragraphs.

Design 1. - In this design the fuel-emitter piece of each diode is fixed on one end while the other end is free to grow axially. The arrangement of the components is shown in figure 26(a). In order to contain the cesium, the series lead functions as a seal in addition to being an electrical lead and an expansion joint. The fixed end of the fuel-emitter piece has to be electrically insulated from its collector and the series lead.

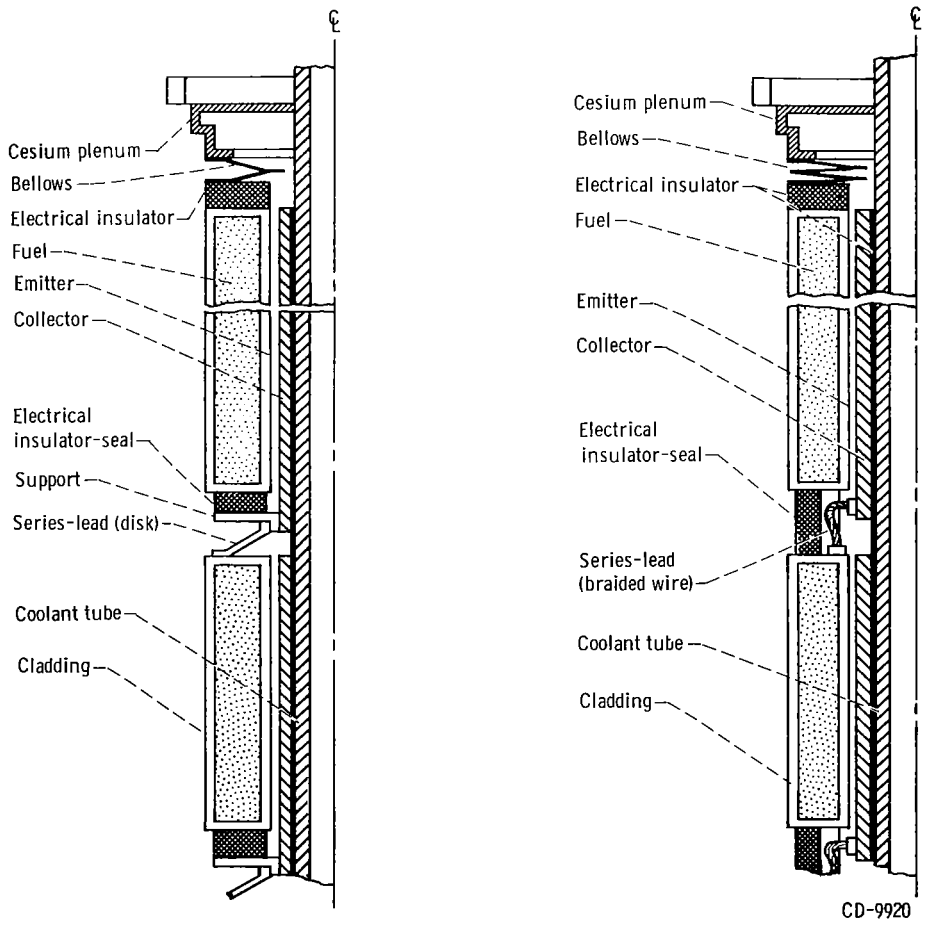

(a) Design 1.

(b) Design 2.

Figure 26. - Insulator-seal designs for vented diodes.

Although they are not shown in the figure, several axial grooves at the joint formed by the collector and the support piece allow the cesium to traverse the fuel element.

The stress problems in the series lead are complicated by the fact that its shape and dimensions are dictated by the diode geometry and the functions it must perform. Essentially, it must be shaped like a conical disk with a central hole where the radial dimensions are limited by the outside diameter of the cladding and the outside diameter of the collector. This shape fixes the heat-transfer and electrical conduction length of the series-lead to the difference between the outside and inside radii. The length could be increased by increasing the cone angle, but this is unsatisfactory for two reasons: (1) It would increase the axial spacing between diodes, which would increase the core size, and (2) it makes the disk more rigid because the load on it becomes more of a compressive load and less of a bending load. Furthermore, the disk thickness increases as the length increases adding to the rigidity. The thickness increases because the length to cross-sectional area ratio of an optimum series lead is a constant value (see the section Internal Ohmic Losses). Since this area is the disk thickness times the mean disk diameter, only the disk thickness can increase because the mean diameter is unaffected by the cone angle. Therefore, the dimensions of the series lead for this design are as follows: outside diameter, 2.28 centimeters (0.898 in.); inside diameter, 1.2 centimeters (0.472 in.); and wall thickness, 0.010 centimeter (0.004 in.).

Since the series lead is in contact with the 2000 K (3600° R) emitter, the material must be a refractory metal, such as a tungsten alloy. The differential axial growth between the emitter and its collector causes a deflection in the series lead of 0.008 centimeter (0.003 in.) which stresses it beyond its yield point at temperature. Prediction of failure in the plastic range is difficult to calculate but was approximated in the following manner. Equations for simple beam problems that predict the maximum deflection at the instant of plastic failure are presented in reference 12. The series lead is much like a disk of an expansion bellows which can be considered as a beam (ref. 13). Therefore, it was assumed that the following approximation predicts the maximum deflection of the series lead at the instant of plastic failure:

$$\delta_D \approx \delta_D \frac{\delta'_B}{\delta_B} \tag{12}$$

where

δ'_D maximum deflection of disk (series lead) at instant of plastic failure

δ_D maximum elastic deflection of disk

δ'_B maximum deflection of end-loaded cantilever beam at instant of plastic failure

δ_B maximum elastic deflection of end-loaded cantilever beam

Calculated values of the three deflection terms on the right side of equation (12) result in a maximum plastic deflection of 0.010 centimeter (0.004 in.). Based on the assumptions that led to equation (12), the disk would not fail since its maximum deflection is 0.008 centimeter (0.003 in.). However, stresses due to the radial differential expansion and a thermal gradient of about 555 K (1000° R) were neglected. Therefore, it appears that a design of this type would be marginal at best.

Design 2. - For this design the series lead functions only as an electrical conductor since all 13 emitters of the fuel element are solidly fastened to each other by ceramic insulator-seals (fig. 26(b)). A total differential axial expansion of 0.112 centimeter (0.044 in.) for the fuel element is taken up by a compression bellows at one end of the fuel element. An electrical insulator is installed between the bellows and the last emitter to prevent a short to ground. This electrical insulator is also a thermal insulator which keeps the temperature of the bellows down to about the collector temperature (1400 K) and reduces temperature gradients to negligible values.

The radial dimensions of the bellows are restricted just as the dimensions of the series lead were in design 1. However, the disk thickness can be arbitrarily selected in this case because it affects only the number of disks needed in the bellows. A disk thickness of 0.013 centimeter (0.005 in.) results in a four-disk tungsten-alloy bellows with an outside diameter of 2.28 centimeters (0.898 in.) and an inside diameter of 0.968 centimeter (0.381 in.). The series lead for this design consists of three bundles of fine, braided, tungsten-alloy wires spaced 120° apart. During thermal expansions and contractions these flexible bundles should bend without undue strain.

Design 2 was selected for the reference design for the following reasons:

(1) The reliability of design 1 is questionable from a stress viewpoint.

(2) Design 1 would be more complicated to fabricate.

(3) If one of the joints of the series lead of design 1 were to break, there would be an open circuit. The series lead of design 2 not only provides redundancy, but the braided wires are less likely to fail. Breaking of individual wires would not completely destroy the lead.

(4) If circuit zoning is used, and if the temperature differences between emitters and collectors vary throughout the core due to thermal input variations, equation (2) shows that the series-lead dimensions will vary throughout the core also. The problems associated with design 1 become immediately obvious; but the series lead of design 2 can be altered as required by merely adding or removing wires from the bundles.

However, even design 2 presents problems that require further consideration:

(1) A method of fabrication must be developed to make the compression bellows. Possible methods would include electron beam welding, high-temperature brazing, or an advanced one-piece forming process.

(2) The interelectrode gap may be difficult to maintain for the full core length.

(3) Special jigging devices and assembly procedures must be developed to permit the assembly of one diode at a time. This type of assembly is necessary because the series leads must be installed before the next fuel-emitter piece is welded into place.

(4) More development work must be done on insulator-seal materials because these seals are in contact with the highest-temperature pieces in the core. Only a limited amount of work has been done at this temperature level to date. The graded ceramic - refractory-metal composites seem to be the most promising method of making such insulator-seals. One such candidate that has been fabricated and looks promising for applications to 2000° C is a rhenium - 5 percent yttria and 95 percent stabilized hafnia graded composite (ref. 14).

Summary of Design Data

All pertinent dimensions and other information on the reference design are summarized as follows:

Emitter diameter, cm (in.)	1.25 (0.49)
Emitter length, cm (in.)	2.50 (0.98)
Fuel-element outside diameter, cm (in.)	2.28 (0.898)
Spacing between diodes, cm (in.):	
Radial	0.076 (0.030)
Axial	0.635 (0.25)
Interelectrode gap, cm (in.)	0.025 (0.010)
Cladding thickness, cm (in.)	0.051 (0.020)
Fuel thickness, cm (in.)	0.414 (0.166)
Emitter thickness, cm (in.)	0.051 (0.020)
Collector thickness, cm (in.)	0.090 (0.035)
Trilayer insulator thickness, cm (in.)	0.025 (0.010)
Coolant-tube wall thickness, cm (in.)	0.102 (0.040)
Core length, cm (in.)	45.7 (18.0)
Core diameter, cm (in.)	40.9 (16.1)
Number of core diodes	3276
Number of trielements:	
Zone 1	12
Zone 2	18
Zone 3	24
Zone 4	30
Number of diodes per fuel element	13

Coolant flow rate per fuel element, kg/sec (lb/sec)	0.036 (0.079)
Coolant ΔT, K(^{o}R)	55 (100)
Effective multiplication factor, k_{eff}	1.05
Reflector material	BeO
Reflector thickness, cm (in.)	10.2 (4.0)
Core power output, kW electric	208
Reactor controls	Reflector drums

ELECTRICAL FAILURE PROBLEMS

Electrical failures are of concern not only because of the immediate loss of power, but also because they may propagate additional failures and eventually result in a complete power loss. For example, the remaining diodes of a circuit containing failed diodes may be forced to operate at higher than their maximum design operating temperature which would cause them to fail in turn. The effects of open-circuit and short-circuit failures are studied by using a model circuit composed of 12 trielements in series. To simplify the calculations the following assumptions were used:

(1) The thermal power input of each diode in the circuit is 77 watts per square centimeter.

(2) The current density is constant at 15 amperes per square centimeter.

(3) Unit emitter surface area is used; therefore, current and current density are numerically equal.

(4) The load resistance of the circuit does not change after the failure occurs.

Open Circuit

For this analysis it was assumed that one fuel element of a trielement develops an open circuit. Then there are 11 normal (nonopen) trielements in series with the open-circuited trielements, as shown schematically in figure 27. If the current through the remaining fuel elements of the open-circuited trielements is J_o, the circuit current is $2J_o$. Since the trielements are in series, the current flow through each fuel element of the normal trielements is $2/3\ J_o$.

Since there are diodes per fuel element, the voltage E_N is given by

$$E_N = 143\ v_N \tag{13}$$

where v_N is the individual diode voltage in a normal trielement.

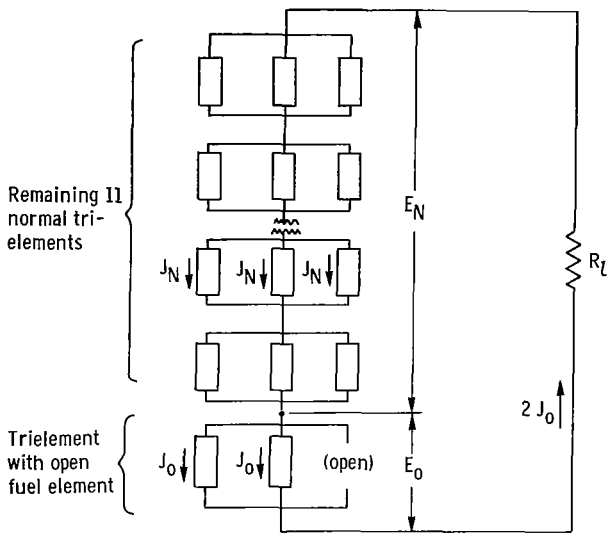

Figure 27. - Schematic of typical reference-design circuit containing open-circuited fuel element.

By the same reasoning, the voltage across the open trielement is

$$E_o = 13\ v_o \tag{14}$$

where v_o is the individual diode voltage in the open trielement.

A prefailure diode voltage of 0.70 volt is obtained from figure 6 (p. 14) with the use of assumptions 1 and 2. The circuit load resistance is the total prefailure circuit voltage divided by the circuit current and its value is 2.42 ohms.

The voltage produced must equal the loop voltage drop so that after the open-circuit failure occurs

$$E_N + E_o = 2J_oR_l = 4.84\ J_o \text{ volts} . \tag{15}$$

By using an iterative procedure and values from figure 6 (p. 14), the final operating points of the diodes in the normal and the open-circuited trielements can be determined. An arbitrary value is assigned to J_N which then fixes J_o, since $J_o = 1.5\ J_N$. The values of v_N and v_o are obtained at the intersection of the $Q = 77$ watts per square centimeter line and proper J-line in figure 6. The voltages E_N and E_o are calculated from equations (13) and (14). The summation of the voltages is compared with the right side of equation (15). If equation (15) is not satisfied, new values of J_N and J_o are chosen, and the process is repeated until equation (15) is satisfied.

The result of this analysis is shown in figure 28. The circle is the operating point of all the diodes before failure. After the open circuit, the diodes in the normal trielements are operating at the power level indicated by the square while the diodes of the open-circuited trielement have fallen to the level denoted by the triangle.

The voltage of a normal diode has risen to 0.72 volt while the current density has dropped to 14.7 amperes per square centimeter. The diodes of the open-circuited trielement are operating at 0.28 volt with a current density of 22.0 amperes per square centimeter. The circuit power loss in this example is about 4.5 percent.

The most important result of this analysis is the fact that the temperatures of most diodes in the circuit have increased beyond their normal operating temperature. Consequently, to ensure long life for the reactor core, the normal maximum operating temperature may have to be reduced. Since the diode efficiencies would drop, the number of diodes and the reactor-core size would have to increase in order to produce the same

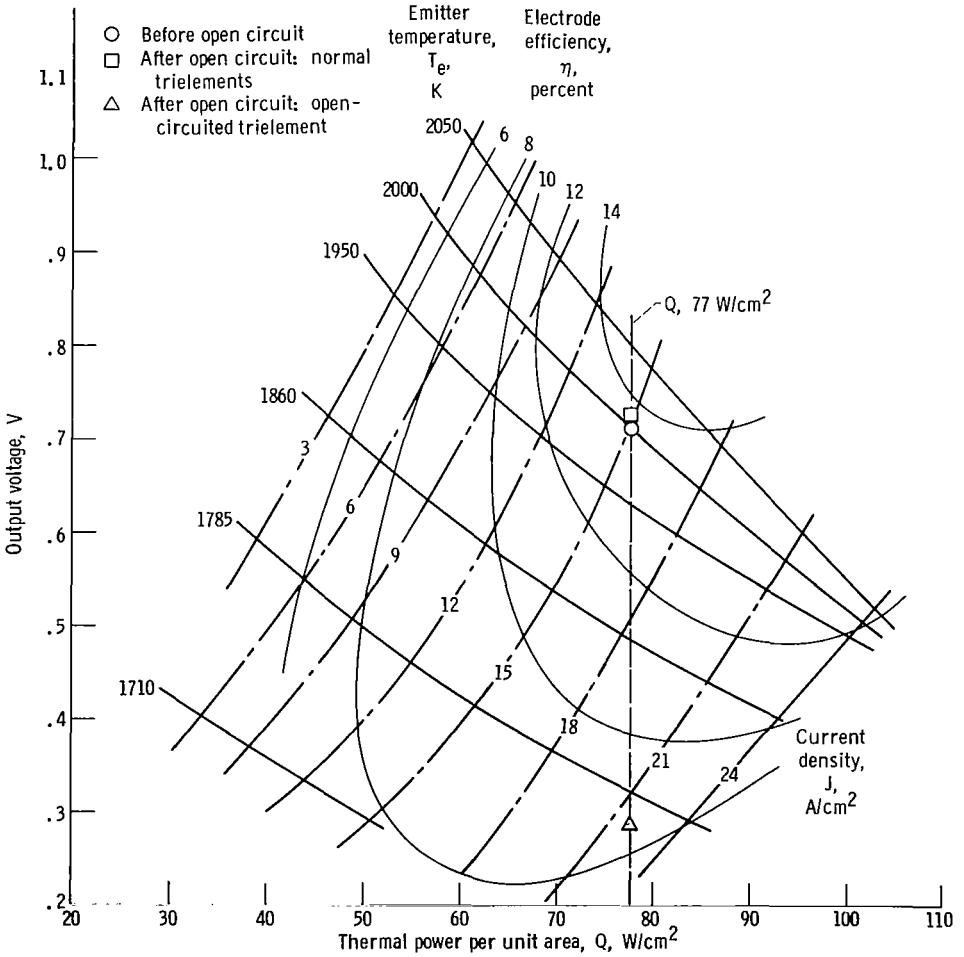

Figure 28. - Open-circuit case with constant input power of 77 watts per square centimeter.

net power. An alternate method of coping with an open-circuit failure would be to reduce the core power when a failure occurs. This method could require a rather elaborate control system which would have to detect the failure, analyze it, and adjust the power accordingly.

Short Circuit

This situation is analyzed by the same method used in the open-circuit case. The circuit shown schematically in figure 29 has 11 normal trielements in series with a trielement containing one short-circuited diode. The two normal fuel elements of the short-circuited trielement are the "a" fuel elements, while the "b" fuel element contains the short-circuited diode. The resistance of the short-circuited diode is neglected. In effect then, the a fuel elements contain 13 diodes each while the b fuel element contains 12 diodes. Since they are in parallel, there is an obvious voltage mismatch for this trielement.

The sum of the current in the short-circuited trielement must equal the circuit current; therefore,

$$3J_N = 2J_a + J_b \tag{16}$$

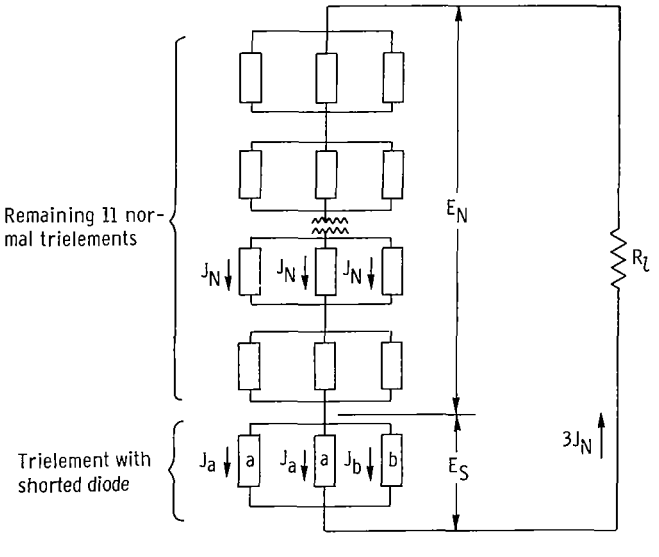

Figure 29. - Schematic of typical reference-design circuit containing one short-circuited diode. (All diodes are operational in "a" fuel element; one diode is short-circuited in "b" fuel element.)

The voltage across the short-circuited trielement is

$$E_S = 13\ v_a = 12\ v_b \tag{17}$$

where v_a and v_b are the individual diode voltages of the a and b fuel elements, respectively.

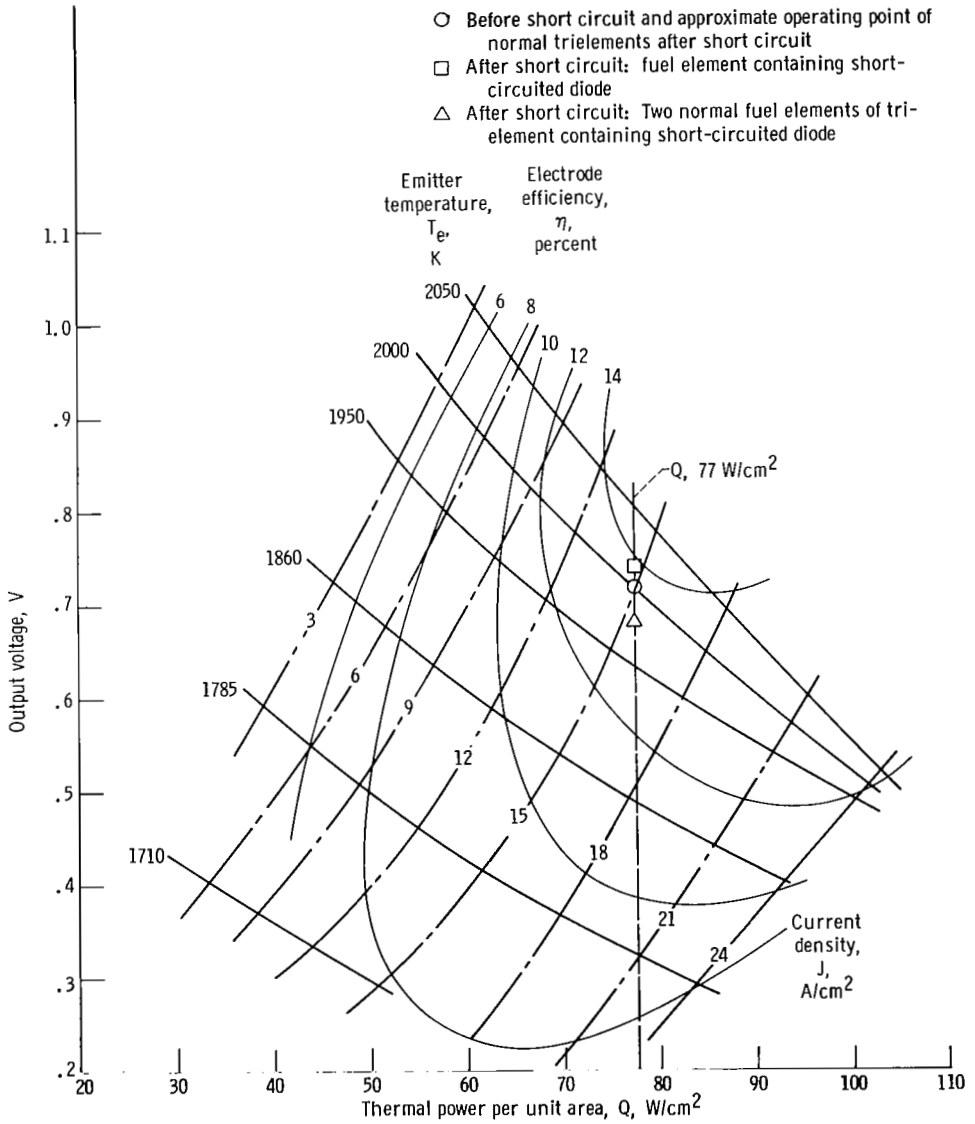

Figure 30. - Short-circuit case with constant input power of 77 watts per square centimeter.

As before, the voltage produced must equal the loop voltage drop, or

$$E_N + E_S = 3J_N R_\ell = 7.3\ J_N \tag{18}$$

where E_N is obtained from equation (13).

The same iterative procedure described in the preceding section yields the results shown in figure 30. Again, the circle is the normal operating point before failure. The square is the operating point of the b diodes, and the triangle is the operating point of the a diodes after failure occurs. The operating point of all the diodes of the normal trielements drops so slightly that they can be considered to be still operating at the pre-failure operating point.

The power loss is so slight in this case that it can be neglected. Unlike the open-circuit case, most of the diodes are actually operating cooler after the failure than before. It is only the operating diodes of the fuel-element containing the short-circuited diode that experience a temperature rise. The worst that can happen is for an open circuit to occur in the b fuel element due to the excessive temperatures. This then becomes the open-circuit case analyzed in the preceding section.

Open-Circuit Temperature Rise

An additional problem associated with an open-circuit failure is the temperature rise of the diode which experiences the failure. With the loss of electron cooling, the remaining modes of heat transfer are forced to dissipate all the fission heat generated in the fuel. The heat-transfer calculations (which are presented in appendix C) only consider the two most important modes of heat transfer: (1) radiation and (2) conduction through the series lead.

Heat-transfer calculations were performed on externally fueled diodes having the criticality determined fuel thicknesses shown in figure 14 (p. 23). It was assumed that the thermal input heat flux was 77 watts per square centimeter and that the collector temperature remained constant at 1400 K. The calculated temperatures which are plotted against emitter diameter in figure 31 indicate that an emitter diameter of 1.30 centimeters (0.51 in.) is about the largest diameter that can be used without a fuel meltdown. In high-powered reactors, where criticality is not a problem, larger emitter diameters can be safely used because the fuel volume can be reduced.

It can be seen from figure 31 that the the tungsten cladding reaches a temperature of 2880 K (5180° R) which is 800 K (1440° R) below its melting point. Although the cladding does have some structural strength at this temperature, there is the possibility that contact can be made with adjacent fuel elements. If contact is made with a fuel element in a

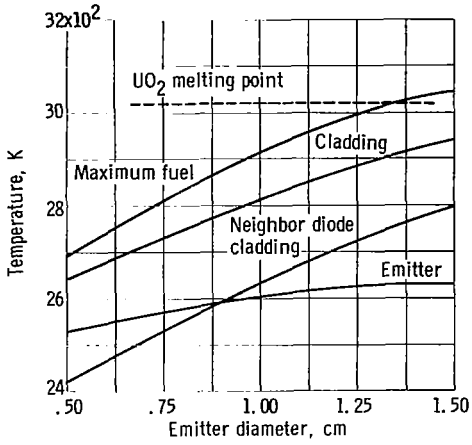

Figure 31. - Open-circuit temperatures as function of emitter diameter for reference-design diode cooled by thermal radiation and by conduction through series lead. Total heat input, 77 watts per square centimeter; heat transferred by radiation, 69.3 watts per square centimeter; heat transferred by conduction through series lead, 7.7 watts per square centimeter; temperature difference through emitter and cladding, 0; collector temperature, constant at 1400 K.

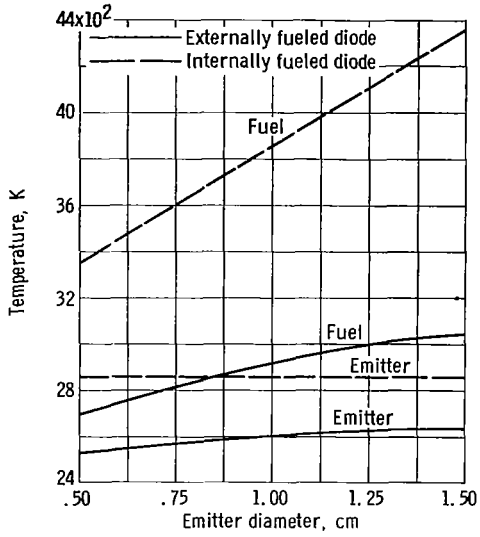

Figure 32. - Comparison of maximum fuel and emitter temperatures of internally and externally fueled diodes for open-circuit case.

different circuit, some of the diodes in that fuel element can be short circuited, resulting in an additional power loss.

The same assumptions were applied to an internally fueled diode in order to make a comparison of the two types of diodes in an open-circuit failure situation. The maximum fuel and emitter temperatures for the two types of diodes are compared on an equal-emitter-diameter basis in figure 32. Although it is impossible for the UO_2 to follow the temperature curve shown for the internally fueled diode (since UO_2 melts at 3020 K), this figure does point out the difference between the two types of diodes. Even for an emitter diameter less than 0.50 centimeter (0.197 in.), the melting point of UO_2 would be reached in the internally fueled diode.

CONCLUSIONS

The following conclusions can be drawn from the preliminary design study of a 200-kilowatt-electric thermionic reactor core composed of short-length externally fueled diodes:

1. The penalties resulting from a nonuniform radial power distribution can be offset by electrical zoning at the expense of electrical complexity. Several radial zones of

fairly uniform thermal power can be established. Each zone operates with a diode current density which corresponds to the maximum power output attainable without exceeding the maximum allowable emitter temperature. About half the power that would be lost by operating all the diodes at the same current density can be recovered by using four radial zones in the reference design.

2. The length of the diode can be optimized to produce the maximum net power per unit volume of reactor core. For the reference-design conditions this length is about 2.0 centimeters (0.79 in.) for a range of emitter diameters of 0.5 to 2.5 centimeters (0.2 to 1.0 in.). The length optimization can be made with good reliability by ignoring the fuel volume.

3. The emitter diameter should be made as small as pumping power and practical problems in manufacturing and assembly allow. This diameter results in the smallest reactor core for any given power level. Also, the reactor size penalty incurred by using larger emitter diameters is more severe for a high-powered reactor than it is for a criticality limited reactor.

4. The radial spacing between fuel elements and the axial spacing between diodes should be made as small as manufacturing and assembly considerations permit in order to obtain the smallest possible reactor core.

5. Increasing the collector thickness decreases the I^2R losses and increases the power per unit cell volume. Coolant pressure drop and overall system weight determine how great the thickness should be for any given emitter size.

6. When an electrical conductor is in parallel with a diode electrode, the conventional electric circuit analysis for parallel conductors yields too low a value for the combined I^2R loss. This result occurs because the current varies along the diode length while the current through the parallel conductor is constant. In the reference design, with the same material and cross-sectional areas for the emitter and fuel cladding, the combined I^2R loss is calculated to be 28 percent higher than the conventional analysis indicates.

7. A limited number of short-circuit electrical failures result in negligible penalties. Open-circuit failures are more serious and require either reduced normal operating temperatures and larger reactor sizes or reduced postfailure power levels.

8. Externally fueled diodes operate with lower fuel temperatures when open circuted than do internally fueled diodes. The reason is that the externally fueled diode has more radiative heat-transfer area and an additional heat sink in its neighboring diodes. To avoid fuel melting in the reference design, the emitter diameter cannot exceed 1.30 centimeters (0.51 in.).

9. Provision for differential axial expansion and sealing the cesium interelectrode space from the fission-gas vent space are difficult and interrelated problems. Both require more thorough analyses, high-temperature materials development, and extensive testing.

Lewis Research Center,
National Aeronautics and Space Administration,
Cleveland, Ohio, May 15, 1968,
120-27-05-20-22.

APPENDIX A

SYMBOLS

A	surface area, cm^2
a	cross-sectional area, cm^2
C_p	specific heat, J/(kg)(K)
D	diameter, cm
E	voltage, V
F	$\frac{3(1-\beta)^2}{\frac{a_w}{a_e}} + 1 - 3\beta + 3\beta^2$
F_V	fuel volume fraction
f	friction factor
g	acceleration due to gravity, cm/sec^2
I	maximum diode current, A
i	variable current, A
J	current density, A/cm^2
K_1	$= \frac{\sigma}{\frac{1}{\epsilon_e} + \frac{1}{\epsilon_c} - 1}$, $W/(cm^2)(K^4)$
K_2	$= \frac{\sigma}{\frac{2}{\epsilon_w} - 1}$, $W/(cm^2)(K^4)$
k	thermal conductivity, J/(cm)(sec)(K)
k_{eff}	effective multiplication factor
L	length, cm
M	fraction of emitter length, cm
N	number of core diodes
N_{Re}	Reynolds number
n	number of diodes in fuel element
P	electrical power, W
$\overline{P}$	average electrical power, W
P_L	electrical power loss, W
p	pressure, N/cm^2
Q	thermal power per unit area, W/cm^2
$\overline{Q}$	average thermal power per unit area, W/cm^2
Q_v	volumetric heat-generation rate, W/cm^3
q	thermal power, W
R	electrical resistance, Ω
S	spacing between diodes or fuel elements, cm
T	temperature, K
t	wall thickness, cm
V	volume, cm^3
v	diode voltage, V
w	mass flow rate, kg/sec
β	$\frac{3 + \frac{a_w}{a_e}}{3 + \frac{2a_w}{a_e}}$
δ	maximum elastic deflection, cm

δ'	maximum deflection at instant of plastic failure, cm
ϵ	emissivity
η	electrode efficiency
σ	Stephan-Boltzmann constant, $W/(cm^2)(K^4)$
ρ	electrical resistivity, Ω/cm
ρ'	density, kg/cm^3
μ	viscosity, kg/(sec)(cm)

Subscripts:

a	normal fuel element of short-circuited trielement
B	end-loaded cantilever beam
b	fuel element containing short-circuited diode
c	collector
D	conical disk with central hole
d	diode
e	emitter
f	fuel
G	gross
g	cesium gap
L	electrical load
l	series lead
m	imaginary plane through fuel
max	maximum
N	normal
o	open circuit
r	radial
rad	by radiation
S	short circuit
s	sink
tot	total
w	fuel cladding
x	axial
1	inside surface of coolant tube
2	outside surface of coolant tube
3	outside surface of electrical insulation
4	outside surface of collector
5	inside surface of emitter
6	outside surface of emitter
7	outside surface of fuel
8	outside surface of cladding

APPENDIX B

OHMIC LOSSES IN ELECTRODES

In a circuit composed of a diode and a load, the current enters the emitter at its maximum value. As electrons are driven from the emitter surface, the current diminishes until it becomes zero at the end of the emitter. If it is assumed that the current density across the interelectrode gap is uniform, the current variation with emitter length is linear, as shown in figure 33. The power loss through the emitter is

$$P_{L,e} = \int_0^{L_e} i^2 \, dR = \int_0^{L_e} I^2 \left(1 - \frac{x}{L_e}\right)^2 \frac{\rho_e}{a_e} \, dx = \frac{I^2 \rho_e L_e}{3a_e} \tag{B1}$$

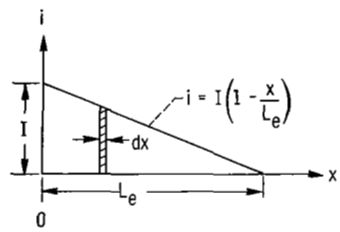

Figure 33. - Assumed current variation along emitter length.

The effective resistance is one-third the resistance of the normal electrical problem where the current remains constant throughout the length of the conductor.

Since the current in the collector builds up from zero to a maximum value as it leaves the collector, the power loss equation is of the same form as equation (B1) or

$$P_{L,c} = \frac{I^2 \rho_c L_e}{3a_c} \tag{B2}$$

The total loss for both electrodes then is the summation of the two losses or

$$P_{L,tot} = \frac{I^2 L_e}{3} \left(\frac{\rho_e}{a_e} + \frac{\rho_c}{a_c}\right) \tag{B3}$$

But $I = JA_e = J\pi D_e L_e$, so equation (B3) becomes

$$P_{L,tot} = \frac{J^2 A_e^2 L_e}{3}\left(\frac{\rho_e}{a_e} + \frac{\rho_c}{a_c}\right)$$

or

$$\frac{P_{L,tot}}{A_e} = \frac{\pi D_e J^2 L_e^2}{3}\left(\frac{\rho_e}{a_e} + \frac{\rho_c}{a_c}\right) \qquad \text{(B4)}$$

Equation (B4) is the same as the approximate equation derived in reference 5 by a different method.

When an additional electrical conductor is in parallel with one of the electrodes, as in the reference design, the two electrodes cannot be treated as normal parallel resistances because the current varies along the emitter length but is constant through the cladding. In figure 34 it is shown that the current I entering the emitter-fuel piece branches off through the emitter and cladding. The current entering the emitter from the series lead has a maximum value of I_e which diminishes to zero somewhere along the emitter length. The current entering the cladding has a value of I_w which is constant along the cladding length since the ceramic UO_2 is treated as a perfect electrical insulator. The current I_w enters the emitter from below and diminishes to zero at the same point that I_e became zero. The problem then is to solve for I_w, I_e, and the power loss through

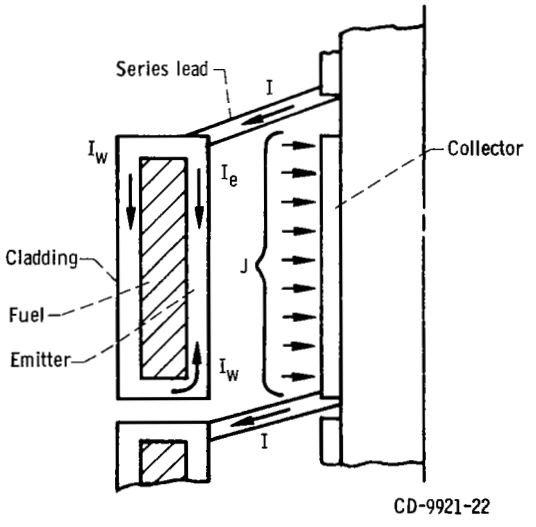

Figure 34. - Current paths through fuel-emitter piece.

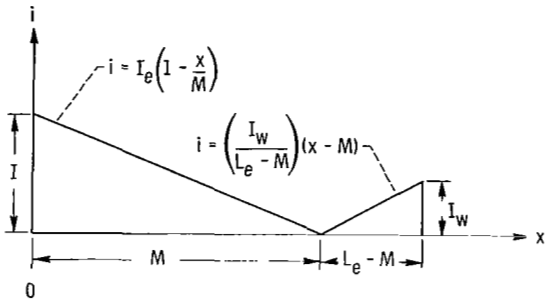

Figure 35. - Assumed current variation along emitter when cladding is in parallel with emitter.

these two conductors. Again, with the assumption of a uniform current density J, the current varies linearly through the emitter, as shown in figure 35. The assumption of a uniform J means that the absolute values of the slopes of the current curves of figure 35 must be equal. That is,

$$\frac{I_e}{M} = \frac{I_w}{L_e - M}$$

or

$$M = \left(\frac{I_e}{I_e + I_w}\right)L_e \tag{B5}$$

Since the sums of the currents in the parallel branches must equal the total current,

$$I = I_w + I_e \tag{B6}$$

In parallel circuits the voltage drops in each branch must be equal. Therefore,

$$I_w\left[\rho_w \frac{L_e}{a_w} + \frac{\rho_e(L_e - M)}{3a_e}\right] = \frac{I_e \rho_e M}{3a_e} \tag{B7}$$

For the special case where $\rho_w = \rho_e$, equation (B7) becomes

$$I_w\left(\frac{L_e}{a_w} + \frac{L_e - M}{3a_e}\right) = \frac{I_e M}{3a_e} \tag{B7a}$$

Combining equations (B5), (B6), and (B7a) results in

$$I_e = \beta I \tag{B8}$$

where

$$\beta = \frac{3a_e + a_w}{3a_e + 2a_w} = \frac{3 + \dfrac{a_w}{a_e}}{3 + \dfrac{2a_w}{a_e}}$$

Substituting equation (B8) into equation (B5) gives

$$M = \beta L_e \tag{B9}$$

and combining equations (B9), (B6), and (B5) gives

$$I_w = (I - \beta)I \tag{B10}$$

Now, the total power loss for the cladding-emitter piece is

$$P_{L,e} = I_w^2\left[\frac{\rho_e L_e}{a_w} + \frac{\rho_e(L_e - M)}{3a_e}\right] + \frac{I_e^2 \rho_e M}{3a_e} \tag{B11}$$

Substituting equations (B8), (B9), and (B10) into equation (B11) gives

$$P_{L,e} = \frac{I^2 \rho_e L_e}{3a_e}\left[\frac{3(1 - \beta)^2}{\dfrac{a_w}{a_e}} + 1 - 3\beta + 3\beta^2\right] = \frac{I^2 \rho_e L_e F}{3a_e} \tag{B12}$$

where

$$F = \frac{3(1 - \beta)^2}{\frac{a_w}{a_e}} + 1 - 3\beta + 3\beta^2$$

Then, the total loss for emitter, fuel cladding, and collector for the special case ($\rho_w = \rho_e$) is

$$P_{L,e} + P_{L,c} = \frac{I^2 \rho_e L_e F}{3a_e} + \frac{I^2 \rho_c L_e}{3a_c} = \frac{I^2 L_e}{3}\left(\frac{\rho_e F}{a_e} + \frac{\rho_c}{a_c}\right)$$

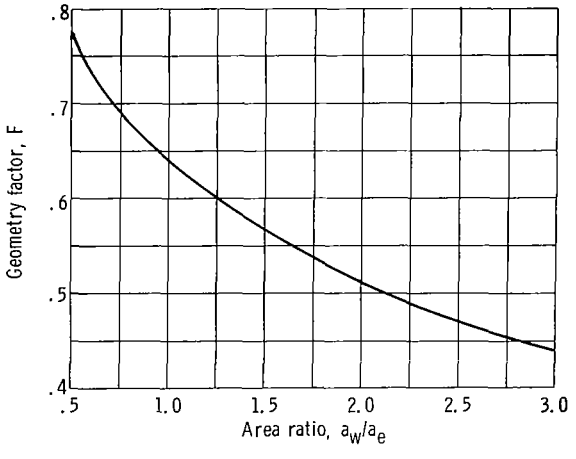

Figure 36. - Variation of geometry factor F with ratio of cladding to cross-sectional areas.

The difference between using equation (B12) and treating the cladding and emitter as parallel conductors in the conventional sense can be illustrated with this example problem. Let the power loss for the normal parallel conductor case be $P^*_{L,e}$. Furthermore, assume that $a_e = a_w$. Then, from figure 36 (where F is plotted against a_w/a_e), F = 0.64. From equation (B1)

$$P^*_{L,e} = \frac{I^2 \rho_e L_e}{3(2a_e)}$$

Then,

$$\frac{P_{L,e}}{P^*_{L,e}} = 2F = 2(0.64) = 1.28$$

Thus, the power loss is 28 percent higher for this particular case than the normal parallel circuit analysis would indicate.

APPENDIX C

OPEN-CIRCUIT HEAT-TRANSFER ANALYSES

When a diode experiences an open circuit, its temperature level rises due to the loss of electron cooling which is a very effective mode of heat transfer. In the heat-transfer analyses presented herein it is assumed that all the heat generated in the nuclear fuel is transferred by thermal radiation and thermal heat conduction through the series lead. Calculations are performed on externally fueled and internally fueled diodes by using the following assumptions:

(1) The thermal input heat flux is 77 watts per square centimeter.

(2) The collector temperature remains constant at 1400 K.

(3) The temperature differences through the emitter and the fuel cladding are neglected.

(4) Axial temperature gradients are neglected.

(5) The fuel thicknesses shown in figure 14 (p. 23) are used for the externally fueled diode calculations.

Two heat-transfer equations from reference 8 are used in the calculations for the externally fueled diodes. The first gives the temperature difference between the outside and inside surfaces of a cylindrical shell with internal heat generation, cooled from the inner surface:

$$T_m - T_e = \frac{Q_v}{16\,k_f}\left[D_6^2 - D_m^2\left(1 - 2\ln\frac{D_m}{D_6}\right)\right] \tag{C1}$$

The second gives the temperature difference between the inside and outside surfaces of a cylindrical shell with internal heat generation, cooled from the outer surface:

$$T_m - T_w = \frac{Q_v}{16\,k_f}\left[D_7^2 - D_m^2\left(1 + 2\ln\frac{D_7}{D_m}\right)\right] \tag{C2}$$

Equations (C1) and (C2) are applied to the externally fueled diode by using the heat-transfer model shown in figure 37. It is assumed that a cylindrical plane of zero thickness and unknown diameter D_m passes through the fuel of the diode. All the heat generated on the inside of D_m is transferred to the emitter and the rest of the heat is

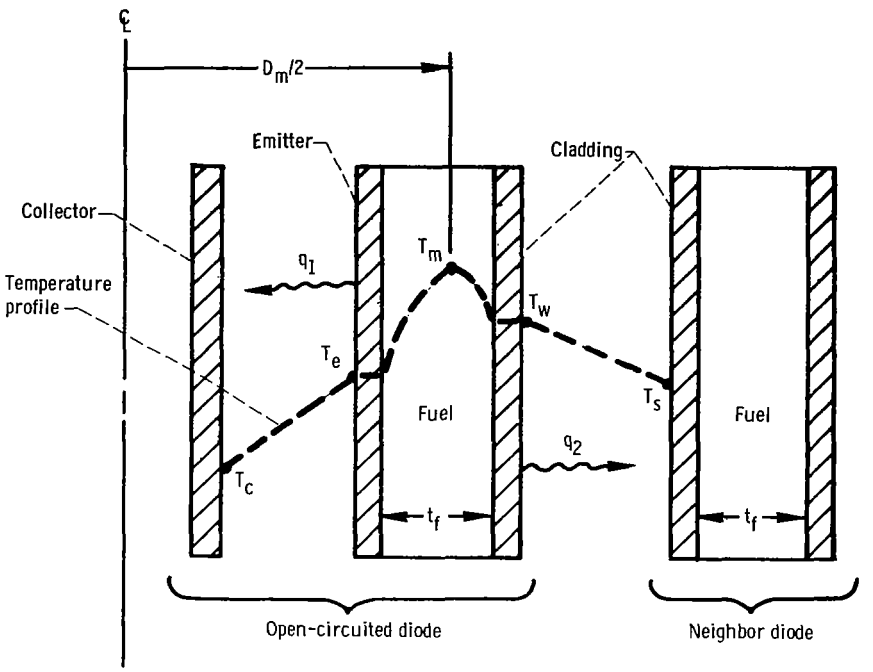

Figure 37. - Model used in heat-transfer analysis of open-circuited externally fueled diode.

transferred to the cladding. Since there are four unknowns and only two equations, more equations are required. The total heat to be removed by radiation is

$$q_{rad} = QA_e = q_1 + q_2 \tag{C3}$$

where the heat transferred by radiation to the collector is

$$q_1 = \frac{\sigma A_e}{\frac{1}{\epsilon_e} + \frac{1}{\epsilon_c} - 1} \left(T_e^4 - T_c^4\right) \tag{C4}$$

and the heat transferred to the neighbor diodes is

$$q_2 = \frac{\sigma A_w}{\frac{2}{\epsilon_w} - 1} \left(T_w^4 - T_s^4\right) \tag{C5}$$

Two more equations are obtained by assuming the volumetric heat-generation rate is uniform throughout the fuel.

$$Q_v = \frac{4q_1}{\pi L_e \left(D_m^2 - D_6^2\right)} \tag{C6}$$

and

$$Q_v = \frac{4q_2}{\pi L_e \left(D_7^2 - D_m^2\right)} \tag{C7}$$

Combining equations (C3) to (C7) and eliminating unknowns yield

$$\left\{ \frac{D_e}{K_2 D_7} \left[Q - K_1 \left(T_e^4 - T_c^4 \right) \right] + T_s^4 \right\}^{1/4} - T_e + \frac{QD_e}{4\,k_f} \left[1 - \frac{2 \ln \left(\frac{D_7}{D_6} \right)}{\left(\frac{D_7}{D_6} \right)^2 - 1} \right] = \frac{K_1}{2\,k_f} D_e \ln \frac{D_7}{D_6} \left(T_e^4 - T_c^4 \right) \tag{C8}$$

where

$$K_1 = \frac{\sigma}{\frac{1}{\epsilon_e} + \frac{1}{\epsilon_c} - 1}$$

$$K_2 = \frac{\sigma}{\frac{2}{\epsilon_w} - 1}$$

The Q term in equation (C8) is that amount of the input heat flux which is dissipated by radiation. The worst case occurs when the total input heat flux is 77 watts per square centimeter. This value is reduced by the amount of heat conducted from the emitter to the collector by the series lead, which is

$$q_l = \left(\frac{ka}{L}\right)_l (T_e - T_c) \tag{C9}$$

For an optimum series lead, equation (C9) becomes

$$q_l = JA_e\left[\frac{k_l \rho_l (T_e - T_c)}{\eta}\right]^{1/2} \tag{C10}$$

As T_e increases, q_l also increases and the Q term of equation (C8) decreases. However, the simplifying and conservative assumption of constant q_l is used. That is, the design temperatures for T_e and T_c are used to give

$$q_l = 7.7\ A_e$$

Then, the amount of heat transferred by radiation becomes

$$q_{rad} = Q_{max}A_e - q_l$$

$$= 77.0\ A_e - 7.7\ A_e$$

$$= 69.3\ A_e$$

So the value of Q used in equation (C8) is 69.3 watts per square centimeter. Equation (C8) is solved iteratively to yield T_e for a given value of D_e, and then equations (C1) to (C7) are used to obtain the remaining unknowns.

The solution of the open-circuit temperature case for an internally fueled diode is straightforward. The difference between centerline and emitter temperature is given by

$$T_{max} - T_e = \frac{Q_v}{16\ k_f} D_f^2 \tag{C11}$$

where

$$Q_v = \frac{QA_e}{\frac{\pi}{4} D_f^2 L_e} = \frac{4QD_e}{D_f^2}$$

which when substituted into equation (C11) gives

$$T_{max} - T_e = \frac{QD_e}{4\,k_f} \tag{C12}$$

The equation for radiation from the emitter to the collector is the same as equation (C4) or

$$q_{rad} = K_1 A_e \left(T_e^4 - T_c^4\right)$$

then

$$\frac{q_{rad}}{A_e} = Q = K_1 \left(T_e^4 - T_c^4\right) \tag{C13}$$

But T_e, the only unknown in equation (C13), is obtained directly to give

$$T_e = 2860 \text{ K (for all } D_e)$$

Now equation (C11) can be solved directly for T_{max}.

REFERENCES

1. Davis, J. P.; Gronroos, H.; and Phillips, W.: Review of Industry-Proposed In-Pile Thermionic Space Reactors. Vol. I: General. Rep. JPL-TM-33-262, Vol. 1, Jet Propulsion Lab., Calif. Inst. Tech. (NASA CR-78331), Oct. 15, 1965.

2. Buatti, A. U.; and Schmitt, J. W.: Design Study of a High Power In-Pile Nuclear Thermionic Space Powerplant. Rep. PWA-2351, Vol. 1, Pratt and Whitney Aircraft (NASA CR-54172), July 30, 1964.

3. Holland, J. W.; and Bosseau, D. L.: Thermionic Converter Network Reliability. Rep. GA-6102, General Atomic Div., General Dynamics Corp., Mar. 19, 1965.

4. Balfour, M. G.; Christensen, J. A.; and Ferrari, H. M.: In-Pile Measurement of UO_2 Thermal Conductivity. Rep. WCAP-2923, Westinghouse Electric Corp. (NASA CR-54740), Mar. 1, 1966.

5. Homeyer, W. G.; and Shanstrom, R. T.: Design Analysis of a Thermionic Reactor. Rep. GA-6845, General Dynamics Corp. (NASA CR-72036), Sept. 22, 1966.

6. Rasor, N. S.: Figure of Merit for Thermionic Energy Conversion. J. Appl. Phys., vol. 31, no. 1, Jan. 1960, pp. 163-167.

7. Kitrilakis, S. S.; Meeker, M. E.; and Rasor, N. S.: Annual Technical Summary Report for the Thermionic Emitter Materials Research Program. Rep. No. 2-63, Thermo Electron Engineering Corp., 1962.

8. Bonilla, Charles F.: An Up-To-Date Review of the Principles of Heat Transfer, with Particular Application to Nuclear Power. Gibbs and Cox, Inc. (AEC Rep. M-4476), 1949.

9. Foster, D. V.: High-Temperature Liquid-Metal-Cooled Reactor Study. Vol. 1. Rep. WANL-PR(R)-002, Westinghouse Electric Corp. (NASA CR-56630), Mar. 1964.

10. Anon.: Conceptual Engineering Design of a 300 KW(E) Thermionic Space Power System. Rep. MNI-CRP-4523, Martin Co., Nuclear Div., Aug. 1962.

11. Lee, Hwa-Ping; and Burton, G. T., Jr.: Thermal Stresses in Three Fundamental Modes of Junction of a Cylinder Sealed to a Disk. Rep. No. 2396, Bendix Corp., Research Lab. Div., Aug. 22, 1963.

12. Faupel, Joseph H.: Engineering Design. John Wiley & Sons, Inc., 1964.

13. Feely, F. J., Jr.; and Goryl, W. M.: Stress Studies on Piping Expansion Bellows. J. Appl. Mech., vol. 17, no. 2, June 1950, pp. 135-141.

14. Dring, M. L.: Ceramic to Metal Seals for High-Temperature Thermionic Converters. The Bendix Corp., Red Bank Div. (RTD-TDR-63-4109), Oct. 1963.

NASA-Langley, 1968 —— 3 E-4294